Reinvestigation of Stauroxylon beckii , a Possible Aneurophytalean Progymnosperm from the Mississippian of France

Thibault Durieux, Anne-Laure Decombeix, Carla J Harper, Jean Galtier

Re-investigation of *Stauroxylon beckii*, a possible aneurophytalean progymnosperm from the Mississippian of France

Thibault Durieux[1*]; Anne-Laure Decombeix[2]; Carla J. Harper[1,2]; Jean Galtier[2]

[1] *Department of Botany, School of Natural Sciences, Trinity College Dublin, Dublin 2, Ireland*
[2] *UMR AMAP, Univ. Montpellier, CNRS, CIRAD, INRA, IRD, Montpellier, France*
**author for correspondence: durieuxt@tcd.ie*

Abstract

Premise of the Research

The fossil record shows that seed plants appeared during the Devonian and started to become dominant in the Mississippian. However, the identity of their closest relatives remains uncertain with three candidates: Stenokoleales, Archeopteridalean progymnosperms, and Aneurophytalean progymnosperms. To clarify the relationships of these groups, it is necessary to document as many Devonian-Missisippian taxa as possible and increase taxon sampling in phylogenetic analyses. In this context, *Stauroxylon beckii* Galtier 1970 from Mississippian deposits of France is particularly interesting because of its similarities with both seed plants and some of their potential closest relatives. Here, we provide an updated description of *Stauroxylon* and discuss its affinities using morpho-anatomical comparisons and phylogenetic analyses.

Methodology

The holotype of *Stauroxylon beckii* and a new specimen from the same formation are described using thin-sections, cellulose acetate peels, and polished surfaces. The morpho-anatomy of the specimens is compared to that of early seed plants and their putative relatives. *Stauroxylon* is also included in phylogenetic analyses of the Radiotopses based on Toledo et al, 2021's matrix.

Pivotal Results

Stauroxylon beckii possess a cruciform protostele with protoxylem strands at the tips of the ribs, a central protoxylem strand, and produces second and third order axes in perpendicular planes. The new specimen differs by characters interpreted as developmental differences or intraspecific plasticity (organotaxis, secondary growth) and is also assigned to *Stauroxylon beckii*. Both comparative approaches and phylogenetic analyses place *Stauroxylon* within the Aneurophytalean progymnosperms, a group previously only known in the Devonian. The inclusion of *Stauroxylon* strengthens previously established relationships within the radiatopsids. *Stauroxylon* also displays structural fingerprints important for leaf and pith evolution.

Conclusions

Stauroxylon is interpreted as a Mississippian representative of the Aneurophytales. It provides new information on the relationships and morpho-anatomical diversity of early seed plants and their closest relatives.

Key-words: Devonian; Carboniferous; lignophytes; radiatopsids; anatomy; phylogeny

Introduction

Understanding the early stages of seed plant evolution in the Devonian and Carboniferous and the identity of their sister group are key research topics in paleobotany. The first occurrence of fossil seeds and vegetative remains with a possible seed plant affinity is a Middle-Late Devonian event (May and Matten, 1983; Rothwell et al., 1989, Gerrienne et al., 2004), and the candidates for their closest relatives are taxa that appeared during the Devonian and disappeared at, or soon after, the end of this period. Three groups have been proposed in the literature, all sharing important morpho-anatomical features with the early seed plants, (1) the Archaeopteridalean and (2) Aneurophytalean progymnosperms and the (3) Stenokoleales, (Matten and Banks 1969; Rothwell and Erwin, 1987; Beck and Stein, 1993; Galtier and Meyer-Berthaud, 1996; Toledo et al., 2018; 2021).

The progymnosperms include three different orders (Beck, 1960b; Beck and Wight, 1988), the Devonian Archaeopteridales and Aneurophytales (Rothwell and Serbet, 1994; Gerrienne et al., 2016; Toledo et al., 2021) and the Carboniferous Protopityales (Beck, 1976; Decombeix et al., 2015). The progymnosperms have been grouped with the seed plants within the Lignophyte division of Crane (1985 "unnamed group" p.720; Doyle and Donoghue, 1986) based on the shared possession of a bifacial vascular cambium producing both secondary xylem and secondary phloem. Unlike seed plants, the progymnosperms all reproduced by spores, with both homosporous and heterosporous representatives (Beck and Wight, 1988). It is still debated (1) whether the progymnosperms are a monophyletic group or a grade, and (2) which one of the three orders is the most closely related to the seed plants. The Protopityales, represented by the single genus *Protopitys*, are unknown in the Devonian, making them too young to be considered good candidates. Arguments to place the Aneurophytales as the closest relatives of early seed plants are mostly related to characters of the stele anatomy (Rothwell and Erwin, 1987), whereas for the Archaeopteridales the evidence is partly based on the reproduction (Beck, 1981).

The Stenokoleales (Matten and Banks, 1969; Beck and Stein, 1993) are an enigmatic Devonian-early Carboniferous family for which only information on the anatomy of main axes and first-orders laterals is known. The anatomy of their distal parts (vegetative or reproductive) and their external morphology remain unknown (Galtier, 2010). Stenokoleales are represented by three genera: *Stenokoleos* (Hoskins and Cross, 1951), *Crossia* (Beck and Stein, 1993), and *Brabantophyton* (Momont et al., 2016a, 2016b). Their stele anatomy is relatively similar to that of the earliest seed plants (Beck and Stein, 1993) and both *Brabantophyton* and *Crossia* possess secondary xylem (Beck and Stein, 1993; Momont et al., 2016a, 2016b), which led some authors (i.e. Matten and Banks, 1969; Galtier and Meyer-Berthaud, 1996; Momont, 2015; Toledo et al., 2018) to suggest a close relationship with the seed plants.

While the Devonian saw the origin of the seed plants, the early Carboniferous (Mississippian) is the period that witnesses the first major diversification of this group (Galtier, 1988 fig 3.1). Among their possible sister groups, the last Stenokoleales are early Mississippian in age (Cross and Hoskins, 1951; Beck, 1960a). The Archaeopteridalean progymnosperms may have crossed the Devonian/Carboniferous boundary (although this is contingent to a revised dating of some "early Tournaisian" deposits, Cross and Hoskins, 1951; Beck, 1981; Beck and Wight, 1988) but there are no Aneurophytalean progymnosperm reported in the Carboniferous. One possible and intriguing exception however is *Stauroxylon beckii,* an anatomically preserved plant from middle Tournaisian (early Mississippian, *ca*. 350 Ma) deposits of the Montagne Noire region in southern France. The original description of *Stauroxylon* (Galtier, 1970) was in French and this taxon has rarely been mentioned in the literature afterwards, despite having an interesting combination of characters, including a cross-shaped actinostele with 5 permanent strands of mesarch protoxylem, and relatively well-developped secondary xylem. Despite a good understanding of the specimen's unique stem anatomy and lateral organs emission, the lack of reproductive structures prevented its assignment to a well-defined group. Galtier (1970) compared *Stauroxylon* with the seed plant *Tetrastichia* (Gordon, 1938, Dunn and Rothwell, 2012), the

Aneurophytalean progymnosperm *Tetraxylopteris* (Beck, 1957; Scheckler and Banks, 1971a), the Archaeopteridalean progymnosperm *Actinoxylon* (Matten, 1968), and the Stenokoleale *Stenokoleos* (Hoskins and Cross, 1951; Beck, 1960a; Matten and Banks, 1969; Beck and Stein, 1993). Galtier (1970) also noted some similarities with the Iridopteridales and Cladoxylales, extinct relatives of the ferns *s.l.* (i.e. Moniliformopses, Kenrick and Crane, 1997; Durieux et al., 2021). Galtier (1970) concluded that *Stauroxylon* was probably a progymnosperm, likely a representative of the Aneurophytales. This hypothesis was later shared by Beck (1976) and by Stein (1982).

Despite its intriguing possible affinities with Devonian Aneurophytales and its well-understood stem anatomy, *Stauroxylon* was never included in phylogenetic analyses. In the current stage of our knowledge, it however seems important to test its relationships, especially since Toledo et al. (2021) showed that the phylogenetic signal between Aneurophytales, Archeopteridales, and Stenokoleales can change under different taxon sampling. It is therefore important to include and test the phylogenetic relationships of *Stauroxylon* in these analyses. In this context, we present here a re-investigation of *Stauroxylon beckii* using the original description of Galtier (1970), new observations and measurements of the holotype, and data from a new specimen from the same deposit. We combine a classical comparative approach and the first inclusion of *Stauroxylon* in a phylogenetic analysis to discuss its affinities in the light of our current understanding of Stenokoleales, progymnosperms, and early seed plants.

Material and Methods

Geological context, fossil preparation and imaging

The holotype of *Stauroxylon beckii* (Galtier, 1970) was found in the Lydienne formation, south-east of the village of St Nazaire de Ladarez in southern France (Hérault).

The Lydiennes Formation corresponds to sedimentary deposits in a shallow sea and consists of alternating beds of argilites and radiolarian cherts containing phosphatic nodules. Horizons containing plant fossils are considered middle Tournaisian in age (Tn2a–Tn2b) based on conodonts (Galtier et al. 1988; Feist et al., 2021). More than 500 specimens representing at least 30 plant taxa have been collected to date in the Lydiennes Formation (Galtier et al., 1988; Decombeix et al., 2020), constituting one of the most diverse plant assemblage of that time period.

The holotype (MN218) was initially analyzed by Galtier (1970) by observing polished surfaces, taking a picture using reflected light with a Ultropak Leitz device, then griding down the polished surface, and repeating the process. This technique is highly destructive because only the photographs remain. On the other hand, it can lead to better observations of the different levels of the plant than using peels or thin-sections. As a result of the destruction of part of the material, some of our reinvestigation is based on the black and white photographs taken by Galtier (1970), via the original 35 mm negative films scanned using a scanner Epson Perfection V850 Pro.

A second specimen (MN 297) found in the Lydienne Formation near Coumiac (Feist et al., 2021: fig 1), had been partially prepared by Galtier who had made 2 thin-sections and 28 acetate peels. For the current study, 72 additional peels were prepared according to standard cellulose acetate peel techniques (Joy et al., 1956; accession numbers: MN 297 B top 2-32, MN 297 C Bot 3-33, MN 297 GL 1-12).

Images from both specimens were taken with a Keyence VX7000 digital microscope at UMR AMAP, France. Some photos were taken with the peel still on the specimen to improve contrast. Images were processed minimally (e.g., brightness and contrast) and converted to greyscale to allow a better comparison with the original images of the holotype taken by Galtier (1970) using Adobe Photoshop version 7.0 (San José, CA, USA). All measurements were made with ImageJ (https://imagej.nih.gov/ij/). Cell diameter measurements are given for the widest dimension unless specified otherwise.

Specimens, slides, peels, and films are part of the Collections de Paléobotanique of Université de Montpellier and are deposited at UMR AMAP, under accession numbers MN 218 (holotype) and MN 297.

Phylogenetic analyses

The phylogenetic analyses, Bremer support, and bootstrapping were conducted using the methodology and the morphological matrix of Toledo et al. (2021:cf. S4: Parsimony analyses). Phylogenetic analyses with parsimony as the optimal criterion were conducted using TNT 1.5 (Goloboff and Catalano, 2016) in Windows 10. The matrix (Appendix A3) used corresponds to the TEA ++ version of Toledo et al. (2021) and includes 50 characters, 9 of them continuous and the others discrete, and 32 taxa, 31 scored by Toledo et al. (2021) and *Stauroxylon beckii*. We scored *Stauroxylon beckii* as a plant possessing a bilateral organotaxis domain *sensu* Toledo et al. (2021). One character in *Tetrastichia bupatides* (C33 = ?) became polymorphic ([1 & 2], i.e. sparganum and dictyoxylon outer cortex) and one in *Laceya hibernica* has been re-scored (Character 1 was corrected from 0.093 -exact same as *T. longii* just above it- to 0.134). Character 4 has also been modified in all the taxa since values for *Stauroxylon* were outside the range of the other taxa, leading to a different value of standardization of this character.

Results

Holotype (MN 218), figs. 1–6

General aspect - *Stauroxylon beckii* is preserved in a 6 cm long phosphatic nodule. The main axis is about 9 mm in diameter. In cross-section, *S. beckii* displays a central cross-shaped actinostele surrounded by secondary xylem and cortex, with conspicuous traces to lateral organs (fig. 1A). The distance between the tips of two opposite ribs of the actinostele is 5 to 6.4 mm. This distance between the tips of the ribs and the general diameter of the axis do not vary much and are relatively uniform along the preserved length of the specimen

Primary xylem- The primary xylem is composed of polygonal metaxylem tracheids (fig. 1A) and parenchyma at the level of the protoxylem (figs. 1B, 1C, 1D). The protoxylem strands are located at the rib tips, with an additional strand in the center of the stele. There are no strands in the midplanes of the ribs (figs. 1B, 1C, 4).

The protoxylem strands have a mesarch maturation and are composed of protoxylem tracheids surrounding parenchyma cells. In cross section, the protoxylem strands at the tip of the ribs are elliptical (about 3 times wider radially than tangentially), 0.25–0.7 mm long and about 0.1 mm wide (fig. 1B), or circular with a diameter about of 160–260 µm (figs. 1C, 1D). Under the circular strands, there is also a poorly preserved tangentially elongated zone of the same cell type (figs. 1C, 1D, at arrowhead) that may also be part of the protoxylem strands. The size and shape of strands may vary during the emission of vascular traces, but it is observed in 5 out of 6 of the cross sections.

The central strand is slightly ellipsoidial, but primarily circular and is about 0.2 mm in diameter (fig. 2A), however, in most sections, the edges of the strand are not clear. Nevertheless, in some instances it appears much larger, about 0.3 to 0.4 mm (see variation in fig. 4). At the base of the specimen, the central strand is four-lobed (fig. 2B) and approximately 0.4 mm in diameter. In longitudinal section, the central strand corresponds to an area of parenchymatous cells and tracheids with reticulate to scalariform pitting (fig. 2C). Unlike in the strands located at the rib tips, protoxylem and parenchyma cells are highly intermixed within this central strand. Protoxylem tracheids are 12–34 µm in diameter (n=50). In longitudinal section, the protoxylem tracheid walls bears reticulate to scalariform pits (figs. 2C, 2D). In the center of the strand, cells with thin walls and polygonal to round shapes are interpreted as parenchyma (fig. 2E). They are wider (14–61 µm, n=50) than the protoxylem

tracheids (fig. 2E) and of various heights (24–120 µm, n=20). Metaxylem tracheids are polygonal, usually larger in their radial dimension, and bigger toward the center of the stele (fig. 1A), leading to cells with disparate sizes ranging in diameter from 14 to 136 µm (n=400). Moreover, these tracheids (which can be partially observed in longitudinal section) are > 3 mm in length according to Galtier (1970). The walls are pitted on all faces. The smallest tracheids have scalariform pitting (fig. 2F), while larger ones have bi- to multiseriate pits that are circular to elliptical in shape and 9–16 µm in diameter (N = 20). These pits are alternate to opposite (fig. 2G). No parenchyma cells were observed in the metaxylem.

Secondary xylem- The secondary xylem is 0.15–0.55 mm in thickness (fig. 1A), and composed of tracheids and rays. In cross section, the tracheids are rectangular to hexagonal, with smaller diameters than those of the metaxylem (15–50 µm, n=50). In longitudinal section, walls are pitted on all faces, typically with scalariform pits (fig. 2H), but a few displays circular bordered pits (fig. 2I). The rays are numerous and parenchymatous. In cross section, they separate 1-8 files of tracheids, but most commonly 2. The innermost ray cells, at the contact with the metaxylem, are larger (fig. 1B, 1C, 1D). In tangential section, the rays are usually uniseriate and 1–3 cells high (fig. 3A). Ray cells are higher than wide (75–35 µm x 15–40 µm, n=12). In radial section, ray cells are rectangular and longer than high (75 µm in height, 150 µm in length, n=1, fig. 3B). Cross-field pitting was not observed.

Phloem–The phloem tissue is reduced (fig. 3E) and rarely preserved. When it is present the cells are poorly preserved. In cross section, the phloem is one to three cells thick and composed of small polygonal cells with thin walls that are 19–58 µm wide (n=20) (fig. 3D). Thin-walled phloem cells that are narrow and elongated in longitudinal section may represent sieve cells (fig. 3C, at arrowhead). There are no conspicuous fibers. Phloem cells seem to be radially aligned (fig. 3D, at arrowhead) suggesting a secondary origin but phloem rays have not been identified.

Cortex–Distal to the phloem, two different cortical zones can be distinguished. They are not easily identifiable in cross section (fig. 3F) but are relatively clear in longitudinal view (fig. 3G). From the center of the stem towards its periphery, the first zone is about 1 mm thick, the second is larger (about 2–4mm) and better preserved.
The first cortical layer is composed of large polygonal cells (40–190 µm wide) with thickened walls. In longitudinal section these cells are more or less rectangular (43–170 µm high and 66–188 µm wide, n=20) and arranged in vertical files (fig. 3G, at black star).
The second cortical layer (figs. 3F, 3G) is formed by cells that are round in cross section, with thickened walls and a highly variable diameter (35–141 µm, n=20). In longitudinal section, these cells are elongated (0.3–1.2 mm long, n=20) and thus easy to distinguish from those of the first zone (fig. 3G).
A third zone composed of smaller cells can be distinguished in some parts of the specimen (fig. 3G), but cells are not clearly different from that the second zone, so we consider this as a simple variation in size of cells from the outer cortical zone.
The axis was likely eroded before fossilization and the epidermis is missing, as could be the most external part of the cortex.

Traces to lateral organs- The central protoxylem strand is not involved in the emission of lateral traces (fig. 4). The emission of vascular traces to lateral organs departing from the tips of the ribs occurs according to a decussate opposite organotaxis (figs. 4, 5). Two traces are emitted at a same level, from two opposite ribs of the primary xylem (figs. 4A, 5A). At the following node, the other two ribs emit traces (figs. 4B–4F, 5B–5F). During the emission, the two opposite traces diverge from the main axis stele at the same speed (fig. 4). Internodes are estimated to be about 18 mm.
The detailed mechanism of a lateral organ emission is presented in the drawings on Fig. 4 and the corresponding pictures in figures 5 and 6. First, the protoxylem strand at the tip of a

rib, which normally has the aspect of a radially elongated lenticular shape with a circle at one end, henceforth referred to as 'buttonhole' shaped (fig. 1B), expands towards the outside (figs. 1C, 1D). A tangential division then gives the strand an overall T-shape (fig. 6A). The radial expansion continues until it has crossed the secondary xylem layer of the main axis (fig. 6B). At that point, the strand that will belong to the departing trace disconnects from the more internal strand, which becomes very reduced (0.2 mm long) (fig. 6B). The protoxylem strand of the stele keeps going straight up and will divide again to produce another second order traces further up. The protoxylem strand of the departing trace continues its tangential elongation (0.75 mm), leading to the formation of two oval strands, which are still linked at the center of the trace (fig. 6C).

In the subsequent stages, the tissues representing the exiting organ individualize completely (figs. 6D–6F) and it becomes triangular (fig. 6D), with the apex pointing towards the main axis (the two traces are about 1–4 mm wide by 0.97 mm high and 1.8 mm wide by 1 mm high; fig. 6D). The tangentially stretched protoxylem seems to form two opposite oval (tangentially elongated) strands with an unclear boundary at the center of the trace making it difficult to establish if these two strands are independent or not (figs. 6D, 6E). At this level the extremity of the rib of the main axis is at a resting phase; the secondary xylem surrounds the metaxylem again and the rib protoxylem strand is buttonhole shaped. The outgoing trace remains devoid of secondary xylem.

During its trajectory in the cortex, the outgoing trace keeps increasing tangentially (2.2–2.5 mm), it expands at its two lateral extremities (fig. 6E), producing an arc shaped, adaxially concave trace (2.5 mm wide) with the protoxylem not particularly abaxial or adaxial but still mesarch. At a higher level, the trace emits two secondary traces perpendicular to the previous plane of branching (fig. 6F). This results in three traces: the circular second order axis (about 1.3 mm wide) accompanied by two small traces of the third order axes, which are emitted in an opposite arrangement in the same plane. The vascularization of these third order axes (fig. 6F, at arrowhead) are viewed in longitudinal section due to the oblique trajectory in the second order axis but they are likely circular in cross section. The vascularization of the second order axes changes from a bilateral symmetry with an adaxial/abaxial polarity in the first stage of emission (triangular and arc shaped) (figs. 4C–4E, 5C–5E, 6D, 6E) toward a radial symmetry after the secondary emission (figs. 4F, 5F, 6F). Due to erosion of the specimen, it is not possible to observe the second and third order axes detached from the main axis and the preservation does not allow to see the location and the number of protoxylem strands in the last stage of the emission.

Specimen MN 297 **(figs. 7–11)**

General aspect - The specimen is preserved in a cone-shaped phosphatic nodule that is about 4.5 cm long and up to 3 cm wide. The specimen has a cross-shaped actinostele, 4.2 to 4.5 mm from one rib tip to the other (fig. 7A). There is no secondary xylem present. The dimensions of the axis do not vary along the nodule, but the overall shape of the stele is twisted in some parts.

Primary xylem - The primary xylem is composed of polygonal metaxylem tracheids without intermixed xylem parenchyma (figs. 7A–7D) and of protoxylem strands located at the center (figs. 7C, 7D, 9) and at the tips of the ribs (figs. 7B, 7H, 9). The mesarch strands at the rib tips are buttonhole shaped, highly elongated and thin (0.3 to 0.8 mm long and 0.05–0.1 mm wide, n=11). They are composed of large parenchyma cells (one cell in width, most of the time) about 28 to 72 µm in diameter (n=30) surrounded by protoxylem tracheids 16–35 µm in diameter, (n=30, fig. 7B).

The central protoxylem strand is more or less circular and composed of a mix of protoxylem tracheids and parenchyma. It can be composed either mainly of parenchymatous cells (fig. 7C) or of protoxylem tracheids (fig. 7D). It is about 0.2–0.3 mm wide (n= 7) with no clear boundary with the surrounding metaxylem. There are no protoxylem strands in the midplane of the ribs.

In cross section, metaxylem tracheids are wider at the center of the stele (17 to 94 µm) than at the rib tips (15 to 43 µm, n=200). The radial diameter of the tracheids at the center of the stele (18 to 94 µm, n=200) is wider than the tangential diameter (17 to 73 µm, n=200), which is not the case for tracheids at the rib's tips. In longitudinal section, the pitting pattern is often poorly preserved. It consists of rounded to scalariform pits about 4.5 to 7 µm wide (n=10)) for the metaxylem (figs. 7E, 7F) and annular thickenings for the protoxylem (fig. 7G). The tracheids pitting was also observed inside a departing trace (fig. 7H, at arrowhead). Longitudinal sections confirm the parenchymatous nature of the cells at the center of the protoxylem strands (fig. 7G).

Phloem - Outside the primary xylem some putative phloem cells have been observed. Their identification is based on their location directly in contact with the primary xylem and their thin walls distinct from those of primary xylem and cortical cells (fig. 8A). In transverse section, these putative phloem cells are oval and elongated tangentially (18–26.5 µm radially, 10.5–18 µm tangentially, n=4). They could not be observed in longitudinal section.

Cortex - The cortex can be separated in two parts. The inner cortex is composed of a few large parenchymatous cells (61–162.5 µm wide, n=22). The outer cortex is composed of smaller cells with thickened walls, polygonal to round-shaped in cross section (46–153 µm wide, n=30) (fig. 8B). In longitudinal section, the two zones are more conspicuous. The inner cortex contains square to rectangular parenchymatous cells 66–184 µm high (n=22) (fig. 8C, at black stars), while the outer cortex contains elongated cells (220–820 µm high, n=30) of collenchymatous or sclerenchymatous nature (fig. 8C, at white stars).
A final outer layer with a badly preserved single layer of cells is found in some part of the specimen and presumably corresponds to the epidermis (fig. 8D). Its cells are oval in transverse section and about 20 to 35 µm (n=5).

Traces to lateral organs- The trace emission pattern can be followed vertically from one extended trace at the bottom of the specimen towards a similar one from the same rib at the top of the specimen. Between these two emissions from a same rib, the specimen emits traces from the 3 other ribs in a more or less simultaneously, giving a triangular shape to the whole specimen. In these two patterns (i.e. 1 vs 3. simultaneous emissions), the mechanism of trace emission from each rib looks similar. It starts with the tangential division of parenchyma cells at the radial tip of the buttonhole strand (fig. 11A). Then, the inflated tip of the protoxylem strand detaches radially from the other part. This emitted strand is circular and made of a few big parenchyma cells (fig. 11B). The trace is also circular when it detaches from the rib of the main axis, with a large, rectangular, central protoxylem strand (fig. 11C). It then divides tangentially, becoming oval with still a large band of protoxylem in its midplane (fig. 11D) that may split to form two mesarch strands (fig. 11E). Later this oval trace emits two secondary traces tangentially. They are poorly preserved but seem to be initially terete (fig. 11F, at arrowhead) and the second order axis becomes more or less circular after emitting them.
While the mechanism of individual trace production is simple, the unusual organotaxis of this specimen combined with the bad preservation of some portions, make a clear understanding of the general pattern challenging. It seems to be composed of two different phases. First, one second order axis is emitted from a rib of the main axis (figs. 9A, 9F–9I, 10A, 10E, right rib). This second order axis emits two secondary traces tangentially (figs. 9I, 10E, 11F right rib). During this first phase, three other second order axes are emitted almost simultaneously from the three other ribs of the main axis, but they remain close to the stele until the first trace is completely free. That is the beginning of the second phase (figs. 9B–9E), where the three traces start moving out, giving a triangular outline to the specimen. During this second phase, the trace located opposite the one emitted during the first phase is the first to be farthest from the stele. Its change to a more circular shape (fig. 9E, left emission) after an

initial tangentially elongated shape suggests that it may have produced a secondary trace that could not be observed due to poor preservation. The two other second order axes seem to remain tangentially elongated for a longer time (figs. 9D–9E, upper and bottom emission).

Systematic palaeobotany

The diagnoses have been translated from Galtier (1970). Crossed text correspond to information that was deleted from the original diagnose and bolded text to information that was added.

Division: Tracheophyta Cavalier-Smith, 1998
Subdivision: Euphyllophytina Kenrick et Crane, 1997
Infradivision: Radiatopses Kenrick and Crane, 1997
Order: Aneurophytales Beck, 1957
Genus: *Stauroxylon* Galtier 1970 Emended Durieux, Decombeix, Harper and Galtier.

Generic diagnosis: anatomically preserved axis bearing opposite decussate ~~branches~~ ~~(~~2nd order axes~~)~~: the latter bear, ~~apparently in a similar fashion, third order axes~~ **two opposite third order axis in a perpendicular plane to the previous level of branching**. The main axis has a cross-shaped protostele (actinostele). Primary xylem has 5 mesarch strands of protoxylem: a central strand and one at the extremity of each rib. **The metaxylem tracheids are larger in their radial dimension, and bigger at the center of the stele.**
Each trace to a second order axis is emitted by a single rib. Outgoing trace triangular **proximally**, produced after tangential division of trace's protoxylem strand, **becoming arc-shaped and adaxially concave before** dividing in three mesarch strands apparently circular and with a radial structure: two small traces (third order axes) surround the strand of the second order axis. Secondary xylem **sometimes present** ~~only~~ at the level of the central stele of the main axis. Protoxylem with parenchymatous elements. Inner ~~bark~~ **cortex** parenchymatous. ~~Middle and outer~~ ~~(?)~~ **Outer** ~~bark~~ **cortex** collenchymatous or sclerenchymatous.

Type species: *S. beckii* Galtier 1970 Emended Durieux, Decombeix, Harper and Galtier

Specific diagnosis: similar to the genus. Main axis circular to elliptical, 9 mm of average diameter. ~~Main branch~~ **Second order axis** 4 mm at the base. Free second and third order axes not preserved. Stele of the main axis cross-shaped: 6 mm in diameter. Central protoxylem larger at the base (0.4 mm). Protoxylem of the ribs buttonhole shaped (0.35 x 0.1 mm).
Metaxylem tracheids **20 to 140 µm wide** with circular or elliptical , bi to multiseriate or scalariform pitting. Secondary xylem (~~0.3-0.5mm thick)~~ **up to at least 0.5 mm when present**. Tracheids smaller **(10 to 50 µm)** than those of the metaxylem, with scalariform pits on all walls.
Rays small **and numerous**, uni to biseriate, of reduced height **(1– 3 cells).**
Inner ~~bark~~ **cortex** (0.6 mm wide) with parenchymatous cells **(40 to 190 µm wide).**
~~Middle and outer~~ Outer ~~bark~~ **cortex** (1–3 mm) collenchymatous ~~or~~ **to** sclerenchymatous with fusiform cells, highly variable in diameter **(50 to 150 µm wide).**
Outgoing trace first triangular (1.3 then 2.2 mm tangentially), producing two small opposite circular strands (0.5 mm) going to the two third order axes
Vascularisation of the ~~primary ramification~~ **second order axis** more or less circular (1.1 x 1.5 mm in diameter)
Internode 18 mm.
Holotype: ~~specimen G 218 Coll. Lab. Paléobotanique, Fac. Sciences, Montpellier~~.
Specimen MN 218 (ex number G 218), Collections de paléobotanique, Université de Montpellier, France.

Formation: ~~nodule in the~~ Lydienne Formation ~~near St. Nazaire de Ladarez~~, Hérault, France. Age: Early Carboniferous. ~~Visean~~ **Tournaisian**

Phylogenetic analyses

The analysis using the Toledo et al. matrix TEA ++ without continuous characters resulted in 208 most parsimonious trees (length 110, RI = 0.587, CI = 0.436). The strict consensus tree does not have a lot of resolution (fig. 12A). Nevertheless, it recovers *Armoricaphyton* as sister to all the other taxa of the analysis, which are included in a large polytomy with only 3 clades resolved. One contains the two Archaeopteridalean genera, *Archaeopteris* and *Actinoxylon.* The second clade (named *Cairoa*'s clade hereafter) includes *Cairoa* in the first derived position and *Stauroxylon* sister to the Aneurophytalean progymnosperms *Proteokalon – Tetraxylopteris*. The last clade includes the early seed plant *Tristichia tripos* sister to a polytomy that includes all the other early seed plants. The rest of the polytomy includes the Stenokoleales, the remaining Aneurophytales, and plants with unclear affinities (e.g., *Yiduxylon*, *Gothanophyton*, *Kenricrana*)

The synapomorphies recovered in the three clades are (1) the presence of a parenchymatous zone at the center of the stele (C49 = 1) for the *Archaeopteris-Actinoxylon* clade, (2) more than 1 distinct order of branching in the radial organographic domain (C11 = <1) for the *Cairoa* group, (3) a sub-opposite organotaxis (C12 = 2) for the group of *Stauroxylon* sister to *Proteokalon - Tetraxylopteris*, and (4) the presence of scattered sclerenchyma in the inner cortex (C29 = 1) for the early seed plant group.

The 50% majority rule tree (Appendix A1) adds resolution. *Kenricrana* and *Gothanophyton* are included in a polytomy sister to all the other taxa except *Armoricaphyton*. The rest of the taxa form a polytomy, including (1) a clade with all the *Stenokoleos* species, (2) three unresolved species: the Aneurophytale *Triloboxylon arnoldii*, and two Stenokoleales species (i.e. *Brabantophyton, Crossia*), and (3) a clade including the rest of the taxa. This last group is made of a polytomy including a clade containing the early seed plants, and the *Cairoa* clade. In addition, *Langoxylon* is sister to *Archaeopteris - Actinoxylon* (Archeopteridales hereafter). *Triloboxylon ashlandicum* is grouped with *Rellimia*, and *Wilhowia phocarum* (Gensel, 1984; 2022) with *Reimannia*.

Additional synapomorphies in the 50% majority rule tree (Appendix A1) include the absence of a central protoxylem strand in Archeopteridales (also shared by the most derived seed plants in the analysis, i.e. *Laceya* and *Tetrastichia*, C17 = 0), and the absence of secondary xylem in the *Stenokoleos* clade.

The analysis using the same matrix with continuous characters results in a single most parsimonious tree (length 128.797, RI = 0.556, CI = 0.424) (fig. 12B). This fully recovered tree adds resolution to numerous polytomies seen in the other analyses but breaks up the monophyly of *Stenokoleos* in a grade that includes *Wilhowia phocarum* as sister to *Stenokoleos holmesii*. However, in this tree, the previously defined groups are all recovered. The Stenokoleales (from *Stenokoleos simplex*'s group towards *Brabantophyton - Crossia* clade) form a grade. *Triloboxylon arnoldii* is basal to *Yiduxylon* (Wang and Liu 2015), which is the taxa sister to a clade including all the other progymnosperms and the early seed plants. Within this clade, the Aneurophytales are resolved as a monophyletic group (excluding *Triloboxylon arnoldii*) that is sister to the Archeopteridales + early seed plants clade.

The Aneurophytales are supported by the presence of terete ultimate appendages (C37 = 1) and the absence of bilaterality, except in *Stauroxylon* (C10 = 0). The synapomorphy of the sister clade of the Aneurophytales, including the Archeopteridales - early seed plant clade is a heterosporous life cycle (note this character is known in only two of the analyzed species; C9 = 1). The group including all the progymnosperms and the early seed plants is supported by a trace divergence pattern involving only one vascular bundle (C42 = 0).

Discussion

Stauroxylon material known to date

Comparison of MN 297 with the holotype – The new specimen MN297 shares many features with the holotype of *Stauroxylon*, especially the organization of its primary vascular system. These similarities include the shape of the actinostele and the location of the protoxylem strands. Both specimens also have protoxylem strands that are buttonhole-shaped with parenchyma at the center and that have comparable sizes even if some strands can be narrower in MN297. The two specimens also share an heterogenous size of metaxylem tracheids, with larger cells at the center and smaller at the rib tips, and both possess radially elongated central tracheids. The cortex of the two specimens has a comparable organization, with an inner part composed of large rectangular cells with thin walls and an outer part composed of smaller cells with thick walls that are elongated longitudinally. Regarding the pattern of trace emission, both specimens produce a single trace to second order axes from a rib tip, and terete traces to third order axis. The two specimens have a central strand that does not divide or seem to be not involved in the production of traces to second order axes. They also display a transition from bilaterality to radial polarity in the same axis order (second order).

On the other hand, there are two conspicuous differences between the specimens. First MN297 does not possess secondary xylem like the holotype. Second, the organotaxis of the second order axes is different: it is clearly opposite-decussate in the holotype, while in MN297 it is more irregular, with a level where three traces are produced at the same node. The early stage of emission is also a bit different, with the formation of a round shape directly after the individualization of the trace in the specimen 297.

Despite these differences, the two specimens are found in the same formation and share several characters of the primary body that are considered systematically significant. It is also interesting to note that no other contemporaneous taxon -from the same formation or elsewhere- has a comparable organization of the stele and lateral organs. In this context, we consider that the observed differences are not enough to warrant the creation of a new taxon for MN297 and we choose to assign it to *Stauroxylon beckii*. The absence of secondary xylem in the new specimen can be explained by the fact that it represents a different part of the plant or developmental stage (as seen in Aneurophytales and Archeopteridales; Scheckler, 1976; 1978). Similarly, a different organotaxis between plants from the same species and even on the same plant can occur during the plant development (Peaucelle et al., 2007), inside the same order of axes (Guédon et al., 2013) and also between axes from different order of branching (e.g., *Actinoxylon*, *Tetraxylopteris*, *Triloboxylon*, *Elkinsia*). The limited length of both the holotype and MN297 prevents us from fully appreciating the regularity of the organotaxis.

Other putative fossils of Stauroxylon - *Stauroxylon beckii* now include two anatomically preserved stems showing the base of lateral organs. One additional specimen (MN896) may exist but it is crushed and extremely difficult to compare with confidence to MN218 and MN297. Other fossils that could potentially belong to this species include an anatomically preserved root from the Lydienne formation (Decombeix et al., 2017) and a compression from coeval deposits of Germany (Meyer-Berthaud and Rowe, 1997). For the root, the affinities have been suggested to be either with *Stauroxylon* or with *Protopitys* based on the secondary xylem tracheids pitting pattern (Decombeix et al., 2017). The compression has a main axis with a diameter and internode length comparable to those of the anatomically preserved holotype, opposite decussate second order axes, and 3 dimensional ultimate appendages (Meyer-Berthaud and Rowe, 1997). However, one important character that is not found in the compression is the quick secondary emission leading to third order branching. The new information on *Stauroxylon* gathered in the present study does not allow us to support or reject the affinities of these two other fossils with

Stauroxylon, even if the compression possesses many important characters in common with the holotype.

Anatomical comparisons with other Late Devonian-Early Carboniferous taxa

Stauroxylon is characterized by an actinostele with a central protoxylem strand and secondary vascular tissues. Devonian-Carboniferous plants with comparable features are the Stenokoleales, the early seed plants, and the Aneurophytalean progymnosperms, presented hereafter from the less to the most similar to *Stauroxylo*n.

Stenokoleales - The Stenokoleales appear in the Middle Devonian and became extinct during the earliest Mississippian (Beck and Stein, 1993). They include 3 genera: *Stenokoleos* (Hoskins and Cross, 1951), *Crossia* (Beck and Stein, 1993), and *Brabantophyton* (Momont et al., 2016a, 2016b). *Stenokoleos* includes 4 species: *S. setchelli* (Hoskin and Cross, 1951), *S. simplex* (Beck, 1960a), *S. bifidus* (Matten and Banks, 1969), and *S. holmesii* (Matten, 1992). The two other genera are monospecific, with the species *Crossia virginiana* (Beck and Stein, 1993) and *Brabantophyton runcariense* (Momont et al., 2016a).

Stenokoleos shares with *Stauroxylon* the presence of an actinostele with mesarch maturation and a central strand. However, the stele of *Stenokoleos* is very different from that of *Stauroxylon*, consisting of 3 or 4 primary xylem ribs that bifurcate at least once. This bifurcation is related to the emission of traces to lateral organs that consist of two traces diverging from a single rib (note that is not known for *S. setchelli* (Momont et al., 2016a)). Nevertheless, *S. bifidus* can also produce a single trace showing an abaxial concavity but, in contrast to *Stauroxylon*, protoxylem strands are numerous and the trace is not triangular at first, but arc shaped (Matten and Banks, 1969). None of the known specimens of *Stenokoleos* has a decussate organotaxis or secondary xylem.

Brabantophyton and *Crossia* share with *Stauroxylon* the presence of an actinostele with mesarch maturation and a central strand, as well as the presence of secondary xylem. Both genera are however highly different from *Stauroxylon*. Their actinostele possess 3 primary ribs that are divided, with numerous protoxylem along each ribs, and traces to second order axes emitted in pairs. In summary, all the representatives of the Stenokoleales known to date differ significantly from *Stauroxylon* in regard to their overall stele organization and their trace emission pattern.

Early seeds plants - The second group of plants that *Stauroxylon* shows morpho-anatomical similarities with is the early seeds plants, an observation already made by Galtier (1970) when he compared his specimen to *Tetrastichia bupatides*.

The late Devonian-early Mississippian actinostelic seed plants have been assigned to several families: the Calamopityaceae, the Buteoxylonaceae, and the Lyginopteridaceae. Some authors also recognize the Elkinsiaceae (Rothwell et al., 1989) and the Tetrastichiaceae (Rothwell et al., 2022). The delimitation of these families is unclear (especially the Lyginopteridaceae (Dunn, 2006)) and their relationships have not been studied from a phylogenetic point of view, likely because of the high amount of missing information and the challenging homologies.

The three genera of Calamopityaceae that possess an actinostele (*Galtiera*, *Bostonia*, and *Stenomyelon)* are highly different from *Stauroxylon*. Those plants do not have a central protoxylem strand, and they possess abundant secondary xylem, a complex trace emission pattern, a spiral phyllotaxis, pitting restricted to the radial wall of secondary xylem tracheids, and *Kalymma*-type petioles, in which one or two traces divide to form four to eight vascular bundles (Stein and Beck, 1978; Beck and Stein, 1987; Galtier, 1988; Meyer-Berthaud, 1984; Meyer-Berthaud and Stein, 1995; Stein and Beck, 1992). Except for the presence of an actinostele in some taxa, the Calamopityaceae have thus few morpho-anatomical characters in common with *Stauroxylon*.

The Buteoxylonaceae includes 3 monospecific genera (C*alathopteris*, *Buteoxylon*, and *Triradioxylon*) (Galtier, 1988). *Calathopteris heterophylla* (Long, 1976) and *Buteoxylon gordonianum* (Barnard and Long, 1973) have a protostele, but they are very different from that of *Stauroxylon*. They possess a "mixed pith" with abundant parenchyma, no central protoxylem, and have a ⅖ phyllotaxy with U-shaped (papilionoid) traces in *Calathopteris* and T-shaped traces in *Buteoxylon*. *Triradioxylon primaevum* shows more similarities with *Stauroxylon,* in particular regarding the location of the protoxylem strands, which are located at the tips of ribs with one or more strands located at the center of the stele (Barnard and Long, 1975). Differences include the presence of a 3 ribbed actinostele, a high amount of secondary xylem with multiseriate and high rays, and a ⅓ phyllotaxis of the fronds with a papilionoid (Y- or T-shaped) trace (Barnard and Long, 1975).

The Lyginopteridaceae include numerous species of late Devonian-Carboniferous age, typically with a *Lyginorachis* type petiole, in which an undivided basal trace that can be butterfly- to U-shaped with multiple abaxial protoxylem strands (May and Matten, 1983; Galtier, 1988). Among the taxa with an actinostele, the less similar to *Stauroxylon* is *Kerryoxylon hexalobatum* (Matten et al., 1984) which possess a six-ribbed actinostele with no central strand, no secondary xylem, and helically born petioles.

Laceya hibernica described by May and Matten (1983) has a 3 ribbed actinostele with protoxylem strands only at the rib tips, manoxylic wood with rays up to 6 cells wide, a ⅓ phyllotaxy, and U-shaped traces.

Tristichia species also have a 3 ribbed actinostele, possess manoxylic wood (Dunn, 2006), and a ⅓ phyllotaxis. Their traces are bilobed to papilionoid, with sometimes two bilobed bundle traces as reported by Galtier and Meyer-Berthaud (1996). One species has been described from the Lydienne Formation (*Tristichia longii*, Galtier, 1977) but the species most similar to *Stauroxylon* is *Tristichia ovensii* (Long, 1961), with a comparable location of the protoxylem strands and a similar shape of one of its early trace emission (cf plate II Figure 17-19, Long, 1961, Figure 2 H-I Galtier and Meyer-Berthaud, 1996). On the other hand, the shape of the stele, the role of the central protoxylem strand in trace emission, and the shape of the trace itself, make *T. ovensii* clearly different from *Stauroxylon*.

Similarities with *Elkinsia polymorpha* described by Rothwell et al. (1989) and by Serbet and Rothwell (1992) and included by some authors in a separate family (i.e. Elkinsiaceae, Rothwell et al., 1989) include the presence of an actinostele with a central protoxylem and pycnoxylic wood. Differences include a 3 ribbed actinostele, the presence of midribprotoxylem strands, and a ⅓ phyllotaxy with variable trace emission (C-shaped, papilionoid, two or four bundles)

Tetrastichia bupatides, also included by some authors in a separate family (i.e. Tetrastichiaceae, Rothwell et al., 2022), is the only early seed plant sharing the 4 ribbed actinostele and an opposite/decussate phyllotaxy (for some specimens) with *Stauroxylon*. Differences include a manoxylic wood, a variable number of xylem ribs in its stele, highly diverse trace formation from butterfly shaped, U- or T-shaped, row or gentle arc (Gordon, 1938; Dunn and Rothwell, 2012; Rothwell et al., 2022). In addition, the trace of *Tetrastichia* when it is close to becoming individualized (see stage D and E of fig 6 Dunn and Rothwell, 2012) has 4 then 8 abaxial protoxylem strand and is surrounded by secondary xylem, which is different from *Stauroxylon*.

The previous comparisons illustrate how, while several taxa of early seed plants show similarities with *Stauroxylon*, none of them share all the important characters. A difference with most of the taxa is the absence of a central protoxylem strand. Another interesting difference is the anatomy of the traces to second order axes in *Stauroxylon* vs. leaf traces of the seed plants. In *Stauroxylon* the concavity of the trace faces the stele and the protoxylem strand is not abaxial or adaxial. Even if some early stages of leaf trace emission in seed plants can have a comparable overall shape (i.e. arc-shaped), they have their concavity towards the outer part of the stem and their protoxylem in an abaxial position (Sanders et al., 2009; Galtier, 2010; Corvez et al., 2012; Momont et al., 2016a).

Aneurophytalean progymnosperms - *The* Aneurophytales were defined as an order of progymnosperms by Beck (1957). They are only known in the Devonian, from the late Eifelian to the Frasnian (372–393 Ma) and had a large geographic distribution (Hammond and Berry, 2005; Meyer-Berthaud et al., 2016). Occurrences of *Rhabdbosporites langii*, a spore found *in situ* in the sporangia of *Tetraxylopteris schmidtii* (Bonamo and Banks, 1967) and *Rellimia thomsonii* (Leclercq and Bonamo, 1971, 1973), suggests a worldwide distribution of the Aneurophytales (Gerrienne et al., 2010).

Anatomically, these plants possess in all their orders of branching an actinostele with 3 to 4 ribs, a central protoxylem strand and at least one protoxylem strand at the tip of each rib (Stein, 1993). When present, other protoxylem strands are located along the midplane of the ribs. Their ultimate appendages are vascularized by a terete strand. Aneurophytales are the first plants to possess secondary vascular tissues produced by a bifacial cambium (Stein, 1993), their secondary phloem contains a lot of thick-walled fibers, and their outer cortex contains a network of thick-walled sclerenchyma cells (Beck, 1976). Aneurophytales have complex pseudomonopodial three-dimensional branching systems, dichotomized ultimate appendages arranged in a spiral or in an opposite-decussate pattern. They are homosporous plants (Gerrienne et al., 2010).

Most Aneurophytales (*Cairoa*, *Triloboxylon* (Matten and Banks, 1966; Stein and Beck, 1983), *Rellimia*, *Aneurophyton*, and *Reimannia* (Matten, 1973) differ from *Stauroxylon* by possessing a three-ribbed actinostele. *Proteokalon* does not have the same number of ribs in its stele depending on the order of branching, so its axes can have either a four-ribbed or three-ribbed actinostele (Scheckler and Banks, 1971b). *Tetraxylopteris* is the only genera to possess a cruciform actinostele similar to *Stauroxylon* in all orders of axes.

Despite important similarities, *Tetraxylopteris* possesses protoxylem strands along the midplane of its ribs (9 strands in total), which is not the case for *Stauroxylon* (5 strands in total). In this regard, *Stauroxylon* is more similar to *Aneurophyton germanicum*, which has one central protoxylem and one strand at the tips of each of its three ribs (Serlin and Banks 1978, but see in Scheckler and Banks,1971b)

In the Aneurophytales, the ultimate appendages traces are terete (Scheckler and Banks, 1971a; Beck and Wight, 1988), and those to the last order of axis are at least three-lobed (Momont, 2015). Thus, the trace emission of *Stauroxylon,* which is triangular to arc shaped with an abaxial/adaxial polarity and becomes more oval-shaped distally (figs. 4C-F), resembles neither that of a next order axis nor that of an ultimate appendage in an Aneurophytales. However, the trace to third order organs and the distal part of the second order axis in *Stauroxylon* are terete, similarly to the ultimate appendages of the Aneurophytales. The opposite taxis of ultimate appendages are present among the Aneurophytales in *Tetraxylopteris*, *Proteokalon* and *Cairoa*, leading to a highly similar emission pattern of the secondary trace in *Tetraxylopteris* and *Cairoa* in comparison to *Stauroxylon*, as can be seen on Beck (1957)'s drawing of *Tetraxylopteris* (especially C and G) and on Stein (1982)'s drawing of *Cairoa*. (Text Figure 2 10, 12). However, *Proteokalon* and *Cairoa* hava a 3-ribbed actinostele when they produce their ultimate appendages and *Tetraxylopteris* still have is cruciform actinostele, and in all of them the branching order that give rise to terete traces does not became terete itself after emitting these traces.

Despite this difference, Aneurophytales species especially *Tetraxylopteris* and *Cairoa* share with *Stauroxylon* the same type of stele with the same arrangement of protoxylem strands, pycnoxylic wood, and a similar organotaxis with the same pattern of secondary trace emission (last order of branching emitting ultimate appendages). These similarities suggest that *Stauroxylon* could be a derived member of the Aneurophytales.

Phylogenetic analyses

The phylogenetic analyses recover a monophyletic group including *Cairoa* sister to *Stauroxylon* (*Proteokalon* - *Tetraxylopteris*) in all the analyses, which is consistent with the conclusion of the above comparative approach suggesting that *Stauroxylon* is closer to the Aneurophytales.

The inclusion of *Stauroxylon* did not change any relationship already shown by Toledo et al. (2021) under the taxon sampling TEA ++, i.e. Stenokoleales as a basal grade, and Aneurophytales as the sister group of the Archaeopteridales - seed plant clade. The implication of these results about taxa placement inside groups, characters evolution, and the tree instability are therefore already described by Toledo et al. (2021). The inclusion of *Stauroxylon* in the matrix decreased the number of maximum parsimonious trees (from 334 to 208) and the resolution of a new group in the analyses without continuous characters. This shows that the inclusion of relatively young taxa (Mississippian in this case) can increase the resolution without changing any phylogenetic relationships.

We also noted that the relationships of *Wilhowia phocarum* changed between the two types of analyses. When only discrete characters are used *Wilhowia phocarum* is found closely related to the progymnosperms in the 50 % majority rule tree (Appendix A1), but when the continuous characters are used it belong to the grade of the Stenokoleales (Fig. 12B). This observation, already seen in trees of Toledo et al. (2018, Appendix 7 vs Figure 1), suggests that the inclusion of this taxon could significantly impact the accuracy of our analyses. Excluding *Wilhowia phocarum* from our analysis with discrete characters (Appendix A2A) decreases the number of most parsimonious trees from 208 to 89, and leads to two new groups in the strict consensus tree, monophyletic Aneurophytales and *Stenokoleos holmesii* as the sister taxa to *S. bifidus*. When excluding *Wilhowia phocarum* plant from our analysis with continuous characters (Appendix A2B), the Stenokololeales appear as a monophyletic group including *Crossia* and *Brabantophyton,* which is consistent with previous classification of these plants (Beck and Stein 1993, Momont et al., 2016a). This Stenokoleales group is also recovered in Toledo et al. (2021) in using 2 different taxon sampling (TEA and TEA+). On the other hand, the phylogenetic position of *Stauroxylon* is independent from the taxon sampling (with or without *Wilhowia phocarum* and from the type of characters used (Figs. 12, S1, S2). Those results tend to show the solidity of the taxonomic placement of *Stauroxylon* in the Aneurophytales.

Evolutionary considerations

Leaf evolution - From a leaf evolution point of view, *Stauroxylon* is interesting because its laterals possess bilateral and abaxial/adaxial polarity at the earliest stage of the trace emission but rapidly become terete distally. This is similar to the situation in the early seed plant *Elkinsia* (Serbet and Rothwell, 1992) but in *Stauroxylon*, this phase of polarity is much more reduced and the abaxial/adaxial polarity seems to be independent of the protoxylem location (i.e. triangular and arc-shaped with protoxylem at the center of the trace). In *Elkinsia*, laterals (i.e. fronds in this case) are terete only distally (Serbet and Rothwell, 1992, Sanders et al., 2009) and the abaxial/adaxial polarity is shown by the abaxial position of protoxylem strands. The polarity of the laterals of *Stauroxylon* could represent an early stage of development towards the abaxial/adaxial polarity of the seed plants, or as implied by its phylogenetic placement in the Aneurophytalean progymnosperms, as another independent evolution of incomplete abaxial/adaxial identity in Lignophytes.

Stele evolution - *Stauroxylon* is also interesting because it possesses wider metaxylem tracheids at the center of the stele than in the ribs, and its central protoxylem strand varies in cell composition, size, and shape. Those variations inside metaxylem and central protoxylem strand is interesting in the context of the discussion on pith evolution and the "*delayed and shortened protoxylem differentiation* hypothesis" put forward by Tomescu and McQueen (2022). This hypothesis involved a modification of the timing of growth and differentiation of the central tracheids leading to the transition from protoxylem/metaxylem toward a central pith. Tomescu and McQueen (2022) also highlight the fact that their hypothesis can be coupled with one of the two hypotheses of Stein (1993) call the hyperinduction scenario when "pith is considered to differentiate in response to the highest

auxin concentrations". In this hypothesis, auxin induces (at least in part) the shortening of the differentiation phase and the increase of the growth period for protoxylem tracheids in *Leptocentroxyla* leading to paedomorphic metaxylem tracheids (i.e. tracheids with reduce wall thickness and "simpler thickening" but with same diameter with the surrounding ones) (Tomescu and McQueen 2022). Auxin flow influencing the timing of growth and differentiation in this way could explain the proto/metaxylem tracheids arrangement of *Stauroxylon*. The parenchymatous center of the central protoxylem strand (figs. 2A, 7C) would be linked to a high concentration of auxin (acting as an inhibitor in this case) in the stele. Then with the distance from the center, the concentration decreases leading to the differentiation of tissues starting with the protoxylem tracheids (at "the highest non-inhibitory auxin concentrations" Tomescu and McQueen, 2022). Surrounding it, the metaxylem, made of large tracheids close to the center, and the most peripherical tissues of this sequence, the narrower metaxylem tracheids in the ribs. These differences of metaxylem tracheids size can be due to the positive influence of auxin (as seen in secondary xylem tracheids of *Pinus* (Larson, 1969; see also Aloni 2021 chap 13 for a review and also the counterargument). We can note that the impact of auxin on the tracheids can also be functioning the other way around with the diameter of the conducting cells increasing with the diminution of the auxin concentration (Aloni, 2021), which in this case is more in line with the hypoinduction hypothesis of Stein (1993). The differences of metaxylem tracheids diameter depending on their position as well as the interchangeability of central protoxylem tracheids toward parenchyma cells, as seen in *Stauroxylon,* tend to confirm the hypothesis of a transition from the central protoxylem strand toward pith formation induce by different auxin concentrations (Stein 1993, Tomescu and McQueen, 2022).

Conclusions

- We redescribe the anatomy of *Stauroxylon beckii*, an early Mississippian plant first described in 1970, based on a reinvestigation of the holotype and on an additional specimen that shows a different organotaxis and lacks secondary growth.
- Classical comparative approaches and phylogenetic analyses suggest a placement in the Aneurophytales, making *Stauroxylon* the youngest representative of this group of progymnosperms previously restricted to the Devonian.
- This discovery highlights once again the high potential of anatomically preserved fossils to understand plant affinities by preserving key diagnostic characters.
- Phylogenetic analyses of radiotopsid recover Stenokoleales as a basal grade sister to the monophyletic Aneurophytales, which are the sister group of the Archeopteridales – seed plants clade. This result is similar to Toledo et al. (2021)'s with the highest taxon sampling and the inclusion of *Stauroxylon* increases the strength of previously recovered relationships.
- *Stauroxylon* is interpreted as displaying structural fingerprints of early stages of leaf and pith evolution: (1) the presence of lateral organs combining an abaxial/adaxial polarity without an adaxial/abaxial placement of the protoxylem strand proximally, (2) size variations of metaxylem tracheids, and a central protoxylem strand variability in terms of size and cell type composition.

Acknowledegments

We thank Mihai Tomescu (Arcata, USA) for his advice on character coding and for facilitating data sharing. We also thank Gar Rothwell and the other, anonymous reviewer for their helpful comments on a previous version of the manuscript. This work is part of TD's PhD project "Early woody plant diversity and biology: An integrative evolutionary and palaeoenvironmental study" funded by a TCD Provost's Award to CJH. This work was also partly supported by a Tellus-Interrvie grant (DECA, CNRS-Institut National des Sciences de

l'Univers) to ALD, and a PHC Ulysses grant (#47212TK, Irish Research Council and French Ministry of Foreign Affairs) to CJH and ALD. AMAP (botAny and Modelling of Plant Architecture and vegetation) is a joint research unit that associates Montpellier University, CNRS (UMR 5120), CIRAD (UMR51), INRAe (UMR931), and IRD (UR123).

Author contributions

TD led the project including the observations, systematic comparisons, and phylogenetic analyses. ALD, CJH, and JG contributed expertise in Devonian-Carboniferous plant anatomy and systematics. All the authors have provided critical inputs and feedback and accepted the final version of the manuscript.

Data availability

All data that support the findings of this study are included in this article and its appendices. The original versions of Figs 1-3, 5, 6-8, and 10-11 (in color) are deposited in Figshares (DOI: https://doi.org/10.6084/m9.figshare.24959736). The fossils, associated slides, and peels are deposited in the Collections de paléobotanique, Université de Montpellier, under specimen numbers MN218 and MN297.

References

Aloni R 2021 The control of tracheid size, vessel widening and density along the plant axis. Pages 223-235 *In* R Aloni. Vascular Differentiation and Plant Hormones. Cham: Springer International Publishing.

Barnard PDW, AG Long 1973 On the structure of a petrified stem and some associated seeds from the Lower Carboniferous rocks of East Lothian, Scotland. Trans. R. Soc. Edinburgh 69:91–108.

———1975 *Triradioxylon*, a new genus of Lower Carboniferous petrified stems and petioles together with a review of the classification of early Pterophytina. Trans. R. Soc. Edinburgh 69:231–250.

Beck CB 1957 *Tetraxylopteris schmidtii* gen. et sp. nov., a probable Pteridosperm precursor from the Devonian of New York. Am J Bot 44:350–367.

——— 1960a Studies of New Albany Shale plants. I. *Stenokoleos simplex* comb. nov. Am J Bot 47:115–124.

——— 1960b The identity of *Archaeopteris* and *Callixylon*. Brittonia 12:351–368.

——— 1976 Current status of the Progymnospermopsida. Rev Palaeobot Palynol 21:5–23.

——— 1981 *Archaeopteris* and its role in vascular plant evolution. Pages 193-230 *in* KJ Niklas. Paleobotany, paleoecology, and evolution. Praeger: New York.

Beck CB, WE Stein 1987 *Galtiera bostonensis*, gen. et sp. nov., a protostelic calamopityacean from the New Albany shale of Kentucky. Can J Bot 65:348–361.

——— 1993 *Crossia virginiana* gen. et sp. nov., a new member of the Stenokoleales from the Middle Devonian of Southwestern Virginia. Palaeontogr Abt B 229:115–134.

Beck CB, DC Wight 1988 Progymnosperms. Pages 1-84 *In* CB Beck. Origin and evolution of Gymnosperms. Columbia University Press, New York.

Bonamo PM, HP Banks 1967 *Tetraxylopteris schmidtii*: its fertile parts and its relationships within the Aneurophytales. Am J Bot 54:755–768.

Cavalier-Smith T 1998 A revised six-kingdom system of life. Biol. Rev. 73:203–266.

Corvez A, V Barriel, J-Y Dubuisson 2012 Diversity and evolution of the megaphyll in Euphyllophytes: Phylogenetic hypotheses and the problem of foliar organ definition. Comptes Rendus Palevol 11:403–418.

Crane PR 1985 Phylogenetic analysis of seed plants and the origin of Angiosperms. Ann. Mo. Bot. Gard. 72:716–793.

Cross AT, JH Hoskins 1951 Paleobotany of the Devonian-Mississippian black shales. J. Paleontol. 6:25:17.

Decombeix A-L, J Galtier, B Meyer-Berthaud, C Prestianni, NP Rowe, CJ Harper 2020 A review of the Early Mississippian anatomically preserved flora from Montagne Noire. In: Botany 2020 - Virtual Botany Conference. Virtuel, United States.

Decombeix A-L, D Letellier, B Meyer-Berthaud 2017 Whose roots are these? Linking anatomically preserved Lignophyte roots and stems from the Early Carboniferous of Montagne Noire, France. Int J Plant Sci 178:42–56.

Decombeix A-L, Galtier J , Prestianni C. 2015. The Early Carboniferous progymnosperm *Protopitys*: new data on vegetative and fertile structures, and on its geographic distribution. Hist Biol 27: 345–354

Doyle JA, MJ Donoghue 1986 Seed plant phylogeny and the origin of angiosperms: An experimental cladistic approach. Bot Rev 52:321–431.

Dunn MT 2006 A review of permineralized seed fern stems of the Upper Paleozoic. J. Torrey Bot 133:20–32.

Dunn MT, GW Rothwell 2012 Phenotypic plasticity of the Hydrasperman seed fern *Tetrastichia bupatides* Gordon (Lyginopteridaceae). Int J Plant Sci 173:823–834.

Durieux T, MA Lopez, AW Bronson, AMF Tomescu 2021 A new phylogeny of the cladoxylopsid plexus: contribution of an early cladoxylopsid from the Lower Devonian (Emsian) of Quebec. Am J Bot 108:2066–2095.

Feist R, J-J Cornée, C Corradini, S Hartenfels, M Aretz, C Girard 2021 The Devonian–Carboniferous boundary in the stratotype area (SE Montagne Noire, France). Palaeobiodivers Palaeoenviron 101:295–311.

Galtier J 1970 Recherches sur les végétaux à structure conservée du Carbonifère inférieur Français. PhD diss. Faculté des Sciences de Montpellier. France.

——— 1977 *Tristichia longii*, nouvelle Pteridospermale probable du Carbonifère de la Montagne Noire. C. r. hebd. Séances Acas. Sci., Ser. D, Sci. Nat. 284:2215–2218.

——— 1988 Morphology and phylogenetic relationships of early Pteridosperms. Pages 135-176 in CB Beck. Origin and evolution of Gymnosperms. Columbia University Press: New York.

——— 2010 The origins and early evolution of the megaphyllous leaf. Int J Plant Sci 171:641–661.

Galtier J, B Meyer-Berthaud 1996 The early seed plant *Tristichia tripos* (Unger) comb. nov. from the Lower Carboniferous of Saalfeld, Thuringia. Rev Palaeobot Palynol 93:299–315.

Galtier J, B Meyer-Berthaud, NP Rowe 1988 Tournaisian plants from the "lydiennes" formation of the Montagne Noire (France). Cour. Forschungsinst. Senckenberg 100:109–117.

Gensel PG 1984 A new Lower Devonian plant and the early evolution of leaves. Nature 309:785–787.

Gensel PG 2022 Partially permineralized adpressions of *Wilhowia phocarum* Gensel gen. et sp. nov., a new basal euphyllophyte from the Lower Devonian Battery Point Formation, north shore of Gaspé Bay, Quebec, Canada. International Journal of Plant Sciences 183:604–629.

Gerrienne P, B Meyer-Berthaud, M Fairon-Demaret, M Streel, P Steemans 2004 *Runcaria*, a Middle Devonian seed plant precursor. Science 306:856–858.

Gerrienne P, B Meyer-Berthaud, H Lardeux, S Régnault 2010 First record of *Rellimia* Leclercq & Bonamo (Aneurophytales) from Gondwana, with comments on the earliest lignophytes. Geol. Soc. Spec. Publ. 339:81–92.

Gerrienne P, T Servais, M Vecoli 2016 Plant evolution and terrestrialization during Palaeozoic times—The phylogenetic context. Rev Palaeobot Palynol 227:4–18.

Goloboff PA, SA Catalano 2016 TNT version 1.5, including a full implementation of phylogenetic morphometrics. Cladistics 32:221–238.

Gordon W T 1938 On *Tetrastichia bupatides* - a Carboniferous pteridosperm from East Lothian. Trans. R. Soc. Edinburgh 59:321–370.

Guédon Y, Y Refahi, F Besnard, E Farcot, C Godin, T Vernoux 2013 Pattern identification and characterization reveal permutations of organs as a key genetically controlled property of post-meristematic phyllotaxis. J. Theor. Biol. 338:94–110.

Hammond SE, CM Berry 2005 A new species of *Tetraxylopteris* (Aneurophytales) from the Devonian of Venezuela. Bot. J. Linn 148:275–303.

Hoskins JH, AT Cross 1951 The structure and classification of four plants from the New Albany Shale. Am. Midl. Nat. 46:684–716.

Joy KW, AJ Willis, WS Lacey 1956 A rapid cellulose peel technique in Palaeobotany. Ann. Bot. 20:635–637.

Kenrick P, PR Crane 1997 Perspectives on the early evolution of land plants. Pages 226-309 in Kenrick P, PR Crane. The origin and early diversification of land plant a Cladistic study. Smithsonian Institution Press: Washington and London.

Larson PR 1969 Wood Formation and the Concept of Wood Quality. Yale Univ. Sch. Forestry Bull. 74: 1–54.

Leclercq S, P Bonamo M 1971 A study of the fructification of *Milleria* (*Protopteridium*) *thomsonii* Lang from the Middle Devonian of Belgium. Palaeontogr Abt B 136:83–114.

——— 1973 *Rellimia thomsonii*, a new name for *Milleria* (*Protopteridium*) *thomsonii* Lang 1926 emend. Leclercq and Bonamo 1971. Taxon 4:435–437.

Long AG 1961 *Tristichia ovensii* gen. t sp. nov. : A protostelic Lower Carboniferous pteridosperm from Berwickshire and East Lothian, with an account of some associated seeds and cupules. Trans. R. Soc. Edinburgh 64:477–489.

——— 1976 *Calathopteris heterophylla* gen. et sp. nov., a Lower Carboniferous bearing two kinds of petioles. Trans. R. Soc. Edinburgh 64:477–489.

Matten LC 1968 *Actinoxylon banksii* gen. et sp. nov.: A Progymnosperm from the Middle Devonian of New York. Am J Bot 55:773–782.

——— 1973 The Cairo flora (Givetian) from Eastern New York. I. *Reimannia*, terete axes, and *Cairoa lamanekii* gen. et sp. n. Am J Bot 60:619–630.

——— 1992 Studies on Devonian plants from New York State: *Stenokoleos holmesii* n. sp. from the Cairo flora (Givetian) with an alternative model for lyginopterid seed fern evolution. Cour. Forschungsinst. Senckenberg147:75–85.

Matten LC, HP Banks 1966 *Triloboxylon ashlandicum* gen. and sp. n. from the Upper Devonian of New York. Am J Bot 53:1020–1028.

——— 1969 *Stenokoleos bifidus* sp. n. in the Upper Devonian of New York State. Am J Bot 56:880–891.

Matten LC, WR Tanner, WS Lacey 1984 Additions to the silicified Upper Devonian/Lower Carboniferous flora from Ballyheigue, Ireland. Rev Palaeobot Palynol 43:303–320.

May BI, LC Matten 1983 A probable pteridosperm from the uppermost Devonian near Ballyheigue, Co. Kerry, Ireland. Bot. J. Linn 86:103–123.

Meyer-Berthaud B 1984 *Stenomyelon* from the Upper Tournaisian of the Montagne Noire (France). Can J Bot 62:2297–2307.

Meyer-Berthaud B, A-L Decombeix, R Dunstone, P Gerrienne, N Momont, G Young 2016 *Tetraxylopteris* Beck emend. Hammond and Berry (2005), the first aneurophytalean genus recorded in Australia. Rev Palaeobot Palynol 224:54–65.

Meyer-Berthaud B, NP Rowe 1997 A Lower Carboniferous plant assemblage from Thuringia (Germany): compressions. Rev Palaeobot Palynol 97:361–379.

Meyer-Berthaud B, WE Stein 1995 A reinvestigation of *Stenomyelon* from the Late Tournaisian of Scotland. Int J Plant Sci 156:863–895.

Momont N 2015 Investigation of basal Lignophyte: the Aneurophytales and Stenokoleales reexamined. PhD diss. Université de Liège, Belgium.

Momont N, P Gerrienne, C Prestianni 2016a *Brabantophyton*, a new genus with stenokolealean affinities from a Middle to earliest Upper Devonian locality from Belgium. Rev Palaeobot Palynol 227:77–96.

Momont N, A-L Decombeix, P Gerrienne, C Prestianni 2016b New information, including anatomy of the secondary xylem, on the genus Brabantophyton (Stenokoleales) from Ronquières (Middle Devonian, Belgium). Rev Palaeobot Palynol 234:44–60.

Peaucelle A, H Morin, J Traas, P Laufs 2007 Plants expressing a miR164 -resistant CUC2 gene reveal the importance of post-meristematic maintenance of phyllotaxy in Arabidopsis. Development 134:1045–1050.

Rothwell GW, DM Erwin 1987 Origin of seed plants: an Aneurophyte/seed-fern link elaborated. Am J Bot 74:970–973.

Rothwell GW, R Serbet 1994 Lignophyte phylogeny and the evolution of Spermatophytes: a numerical cladistic analysis. Syst. Bot. 19:443–482.

Rothwell GW, SE Scheckler, WH Gillespie 1989 *Elkinsia* gen. nov., a Late Devonian gymnosperm with cupulate ovules. Bot. Gaz 150:170–189.

Rothwell GW, MT Dunn, AC Scott 2022 Reconstructing the *Tetrastichia bupatides* Gordon plant; a Devonian–Mississippian hydrasperman gymnosperm from Oxroad Bay, Scotland and Ballyheigue, Ireland. Rev Palaeobot Palynol 296:104551.

Sanders H, GW Rothwell, SE Wyatt 2009 Key morphological alterations in the evolution of leaves. Int J Plant Sci 170:860–868.

Scheckler SE 1976 Ontogeny of progymnosperms. I. Shoots of Upper Devonian Aneurophytales. Can J Bot 54:202–219.

——— 1978 Ontogeny of progymnosperms. II. Shoots of Upper Devonian Archaeopteridales. Can J Bot 56:3136–3170.

Scheckler SE., HP Banks 1971a Anatomy and relationships of some Devonian Progymnosperms from New York. Am J Bot 58:737–751.

——— 1971b *Proteokalon* a new genus of progymnosperms from the Devonian of New York State and its bearing on phylogenetic trends in the group. Am J Bot 58:874–884.

Serbet R, GW Rothwell 1992 Characterizing the most primitive seed ferns. I. A reconstruction of *Elkinsia polymorpha*. Int J Plant Sci 153:602–621.

Serlin BS, HP Banks 1978 Morphology and anatomy of *Aneurophyton*, a progymnosperms from the Late Devonian of New York. Palaeontogr. Am. 8:343–359.

Stein W 1982 The Devonian plant *Reimannia*, with a discussion of the class Progymnospermopsida. Palaeontology 25:605–622.

——— 1993 Modeling the evolution of stelar architecture in vascular plants. Int J Plant Sci 154:229–263.

Stein WE, CB Beck 1978 *Bostonia perplexa* gen. et. sp. nov., A Calamopityan axis from the New Albany Shale of Kentucky. Am J Bot 4:459–465.

——— 1983 *Triloboxylon arnoldii* from the Middle Devonian of western New York. Contr. Mus. Paleontol. Univ. Mich. 26:257–288.

——— 1992 New information on *Bostonia perplexa*—an unusual member of the calamopityaceae from North America. Rev Palaeobot Palynol 72:73–102.

Toledo S, AC Bippus, AMF Tomescu 2018 Buried deep beyond the veil of extinction: Euphyllophyte relationships at the base of the spermatophyte clade. Am J Bot 105:1264–1285.

Toledo S, AC Bippus, BA Atkinson, AW Bronson, AMF Tomescu 2021 Taxon sampling and alternative hypotheses of relationships in the euphyllophyte plexus that gave rise to seed plants: insights from an Early Devonian radiatopsid. New Phytol 232:914–927.

Tomescu AMF, CR McQueen 2022 A protoxylem pathway to evolution of pith? An hypothesis based on the Early Devonian euphyllophyte Leptocentroxyla. Ann. Bot. 130:785–798.

Wang D, L Liu 2015 A new Late Devonian genus with seed plant affinities. BMC Evol. Biol. 15:1–16.

Figures

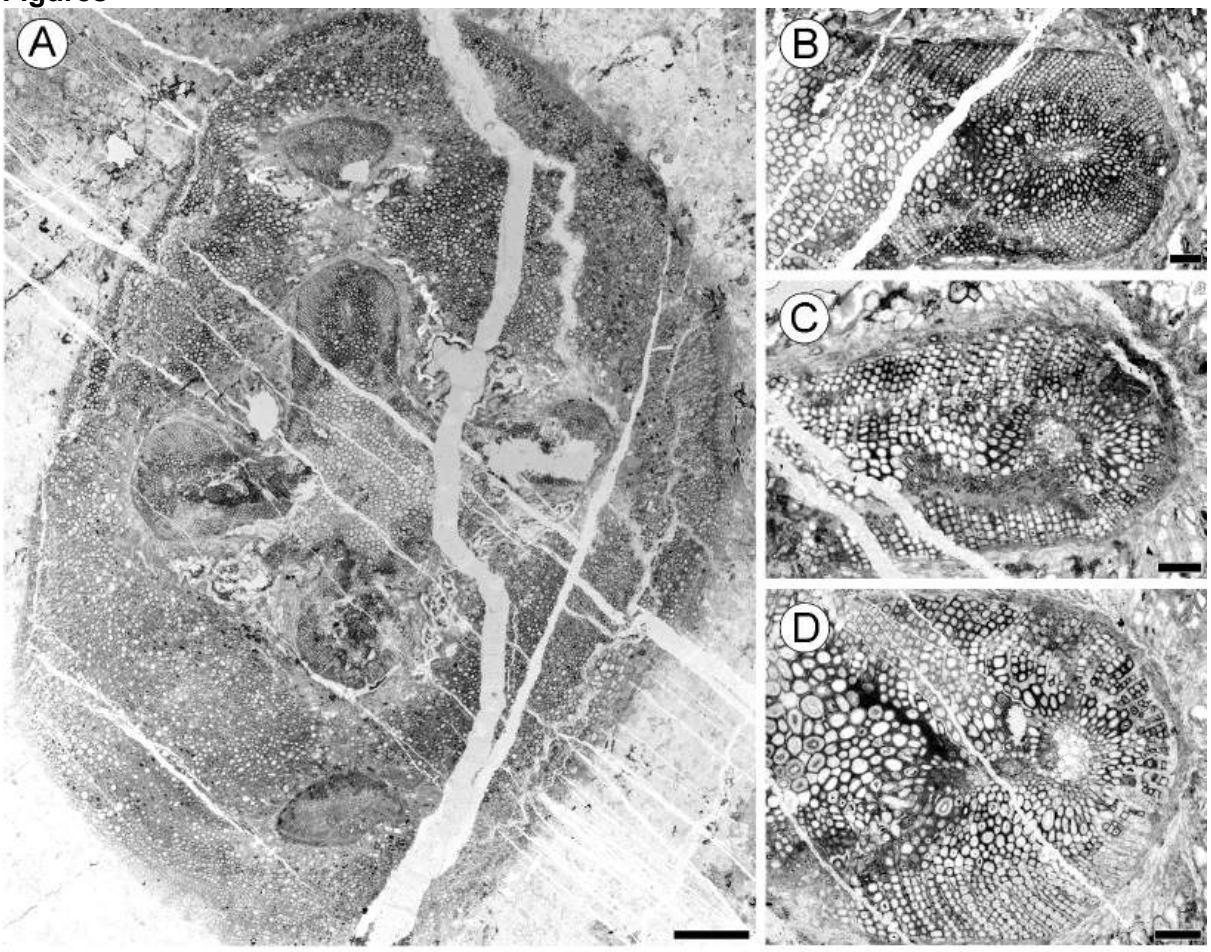

Figure 1: *Stauroxylon beckii*, holotype. General aspect and primary xylem organization. (A) Cross section of main axis showing a cruciform actinostele, secondary xylem, and two opposite traces; scale bar = 1 mm; slide MN218-AI 01; C: Cortex, T: Traces, X1: Metaxylem, X2: Secondary xylem. (B) Buttonhole-shaped protoxylem strand at the tip of a rib; that rib corresponds to the upper rib in A and the right rib of Fig. 4C, 5C; scale bar = 200 µm; slide MN 218-AI 01. (C) Circular protoxylem strand at the tip of another rib (bottom rib of Fig. 4B, 5B) with a badly preserved zone which may be part of the protoxylem strand (arrowhead); scale bar = 200 µm; slide MN 218-BS 02. (D) Circular protoxylem strand at the tip of a rib (upper rib of Fig. 4B, 5B) with a badly preserved zone which may be part of the protoxylem strand (arrowhead); scale bar = 200 µm; slide MN 218-BS 02.

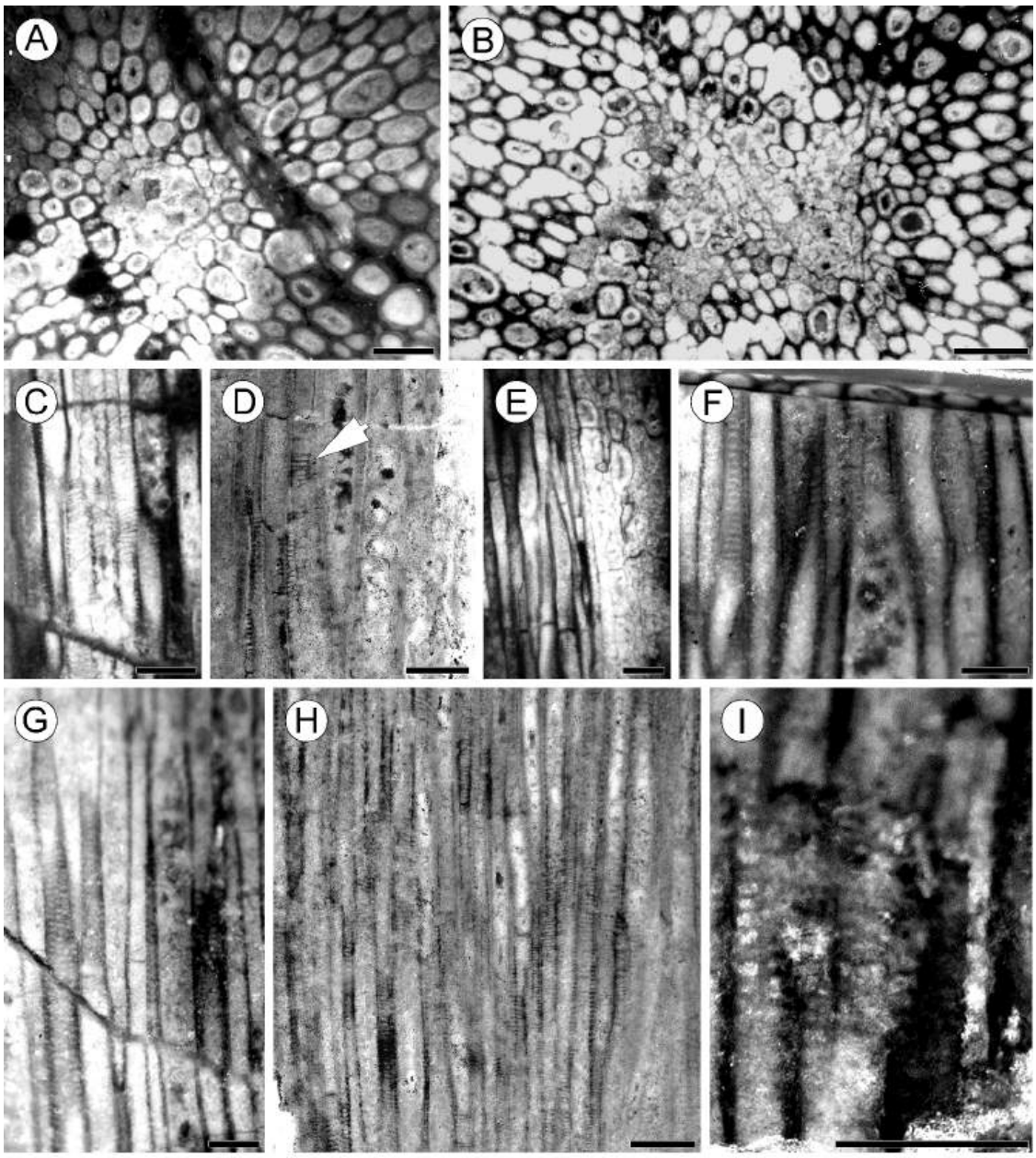

Figure 2: *Stauroxylon beckii* holotype. Primary and secondary xylem anatomy. (A) Central circular protoxylem strand in cross section; scale bar = 100 µm; scan Galtier's film n° 134 (Figure 4 plate 49, Galtier 1970) section MN 218- BL 18. (B) Central four-lobed protoxylem strand in cross section; scale bar = 100 µm; scan Galtier's film n° 104 (Figure 1 plate 50, Galtier 1970) section MN 218-BI. (C) Central protoxylem strand in longitudinal section close to the level of Fig. 1A; scale bar = 100 µm; scan Galtier's film n° 133 (Figure 5 plate 49, Galtier 1970) section MN 218-BL 17; Pr: Protoxylem strand. (D) Reticulate (arrowhead) to scalariform pits of the protoxylem; scale bar = 100 µm; slide MN 218-AL 01. (E) Buttonhole-shaped protoxylem strand in longitudinal section; the parenchyma cell (Pr P: Protoxylem parenchyma) in the right part of the picture and the 3 small tracheids just toward them corresponding to the protoxylem (Pr T); scale bar = 100 µm; scan Galtier's film n° 135 (Figure 5 plate 50, Galtier 1970) section MN 218-BL 18. (F) Scalariform pits on the wall of a small metaxylem tracheid (arrowhead); scale bar = 100 µm; longitudinal section with peel on the specimen 218. (G) Metaxylem tracheid with multiseriate pits (arrowhead); scale bar = 100 µm; longitudinal section with peel on the specimen 218. (H) Secondary xylem tracheids with scalariform pits; scale bar = 100 µm; slide MN 218-AL 01. (I) Secondary xylem with

poorly preserved bordered pits (arrowhead); scale bar = 100 µm; longitudinal section with peel on the specimen 218.

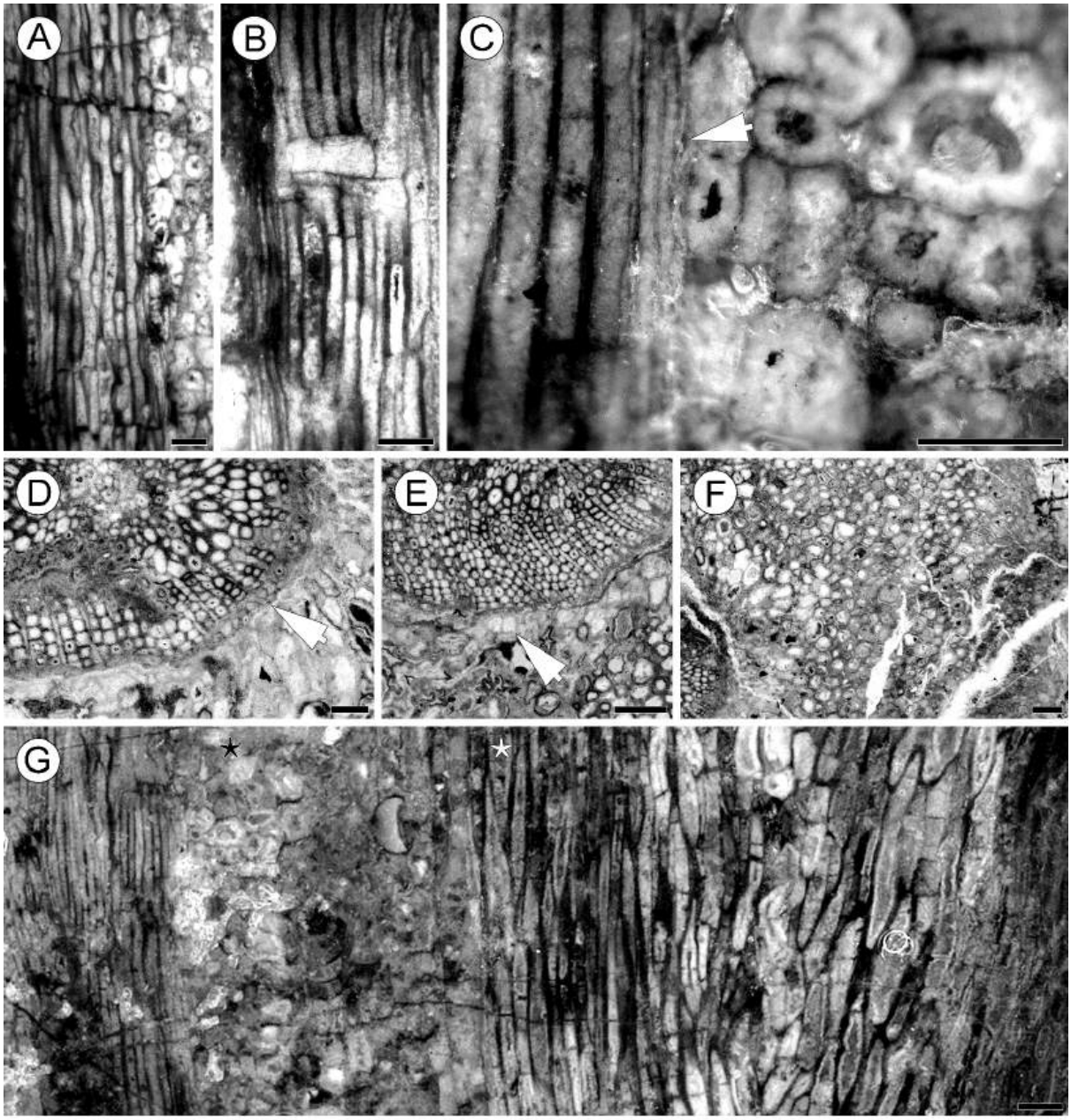

Figure 3: *Stauroxylon beckii*, holotype. Secondary xylem and cortex. (A) Tangential section showing secondary xylem with short uniseriate rays and the inner cortex; scale bar = 100 µm; scan Galtier's film n° 124 (Figure 6 plate 51, Galtier 1970) section MN 218-BL 09; C: Cortex, X2: Secondary xylem. (B) Radial section showing secondary xylem with one ray (R); note the pitting on the radial walls of tracheids; scale bar = 100 µm; scan Galtier's film n°140 (Figure 1 plate 51, Galtier 1970) section MN 218-BL 22-23. (C) Putative phloem sieve cell (arrowhead) in longitudinal section; scale bar = 100 µm; longitudinal section with peel on the specimen 2018. (D) Phloem cells in transversal view; note the arrowhead pointing to three aligned cells, scale bar = 100 µm; slide MN 218-BS 02. (E) Transverse section showing the proximity of inner cortex cell (arrowhead) and the secondary xylem; scale bar = 200 µm; slide MN 218-AI 02. (F) Transverse section of the cortex; scale bar = 200 µm; slide MN 218-AI 02. (G) Longitudinal section of showing the inner cortex (IC) and the outer cortex (OC); scale bar = 200 µm; longitudinal section with peel on the specimen 218.

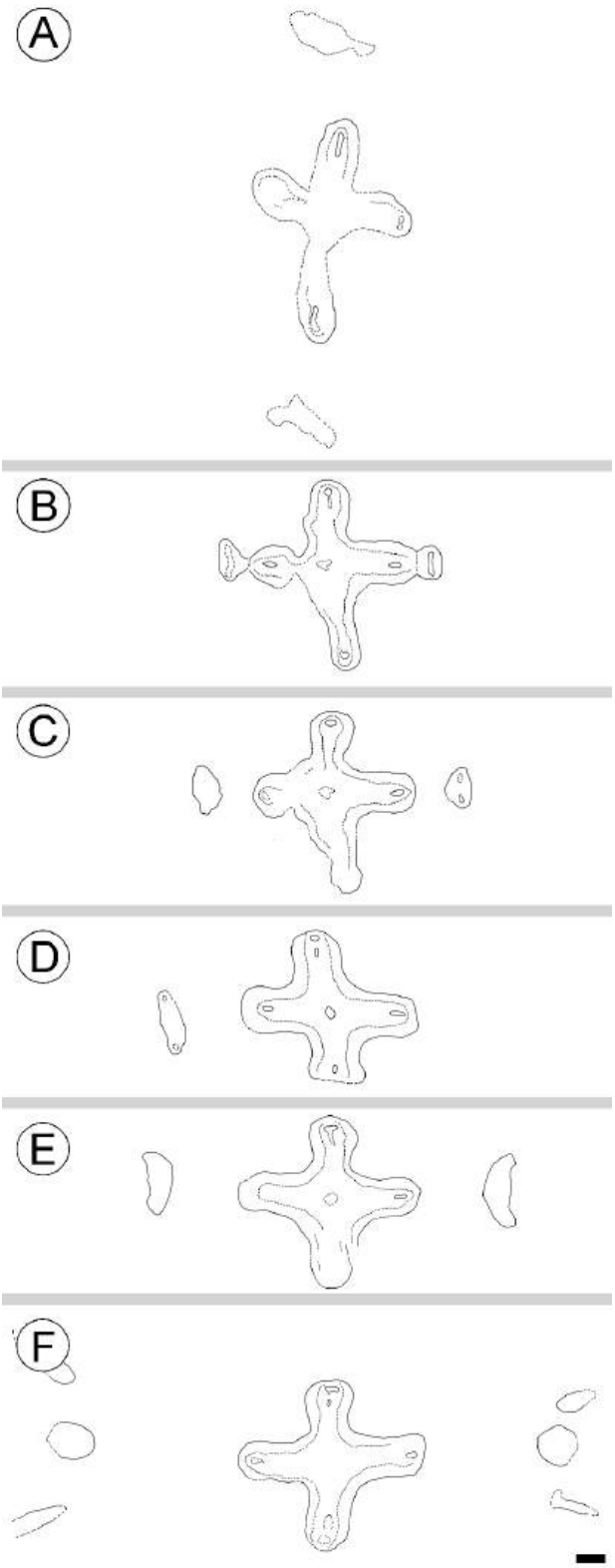

Figure 4: *Stauroxylon beckii*, holotype. Camera lucida drawings of serial transverse sections showing lateral traces emission; scale bar = 1 mm. (A) Slide MN218-BS 04. (B) Slide MN 218-BS 02. (C) Slide MN 218-BS 01. (D) Slide MN 218-AS 02. (E) Slide MN 218-AI 01. (F) Slide MN 218-AI 02; C: Cortex, T: Traces, X1: Metaxylem, X2: Secondary xylem.

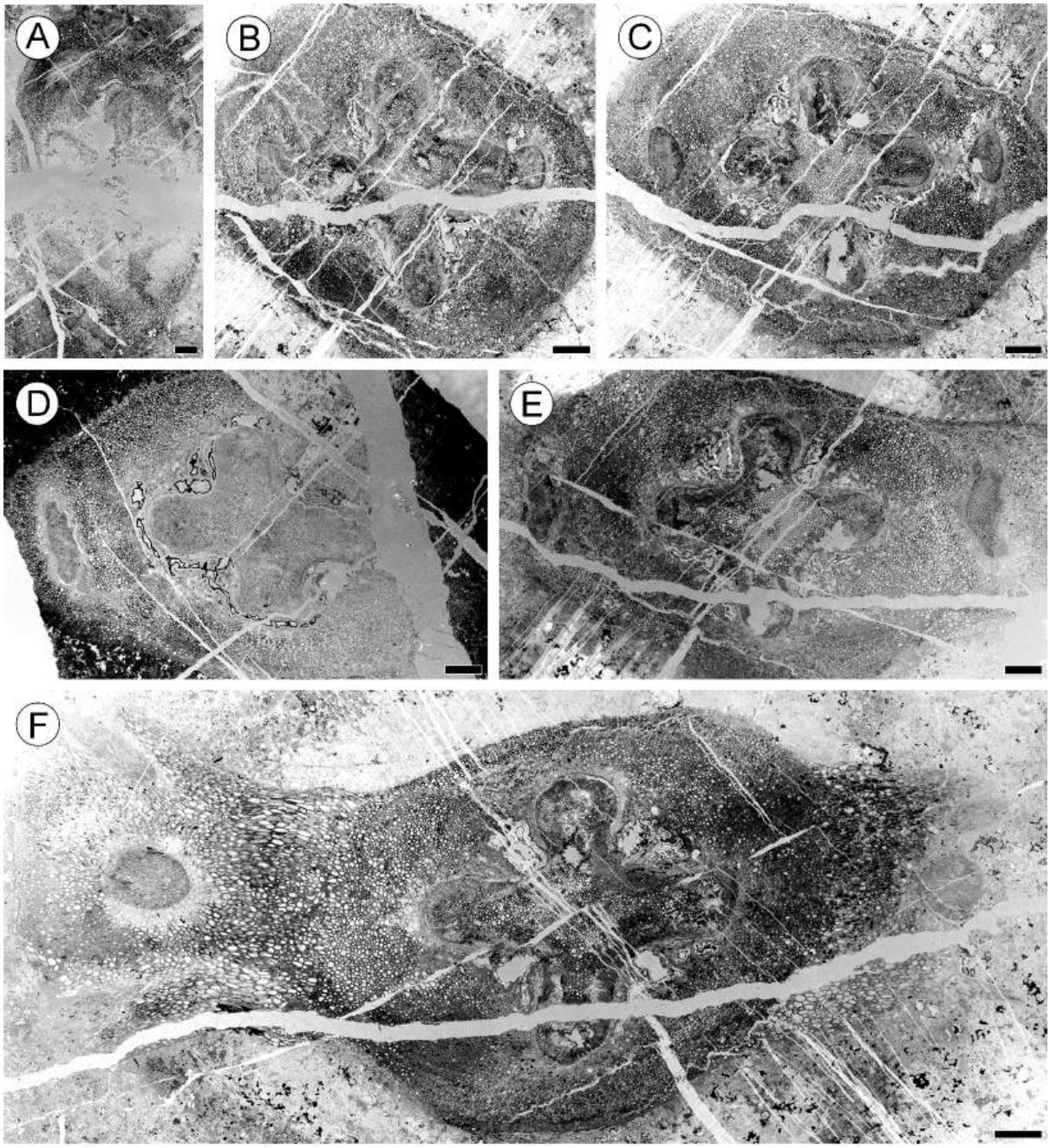

Figure 5: *Stauroxylon beckii*, holotype. Transverse sections corresponding to the drawings on Figure 4; scale bar = 1 mm. (A) Slide MN 218-BS 04. (B) Slide MN 218-BS 02. (C) Slide MN 218-BS 01. (D) Slide MN 218-AS 02. (E) Slide MN 218-AI 01; C: Cortex, T: Traces, X1: Metaxylem, X2: Secondary xylem. (F) Slide MN 218-AI 02.

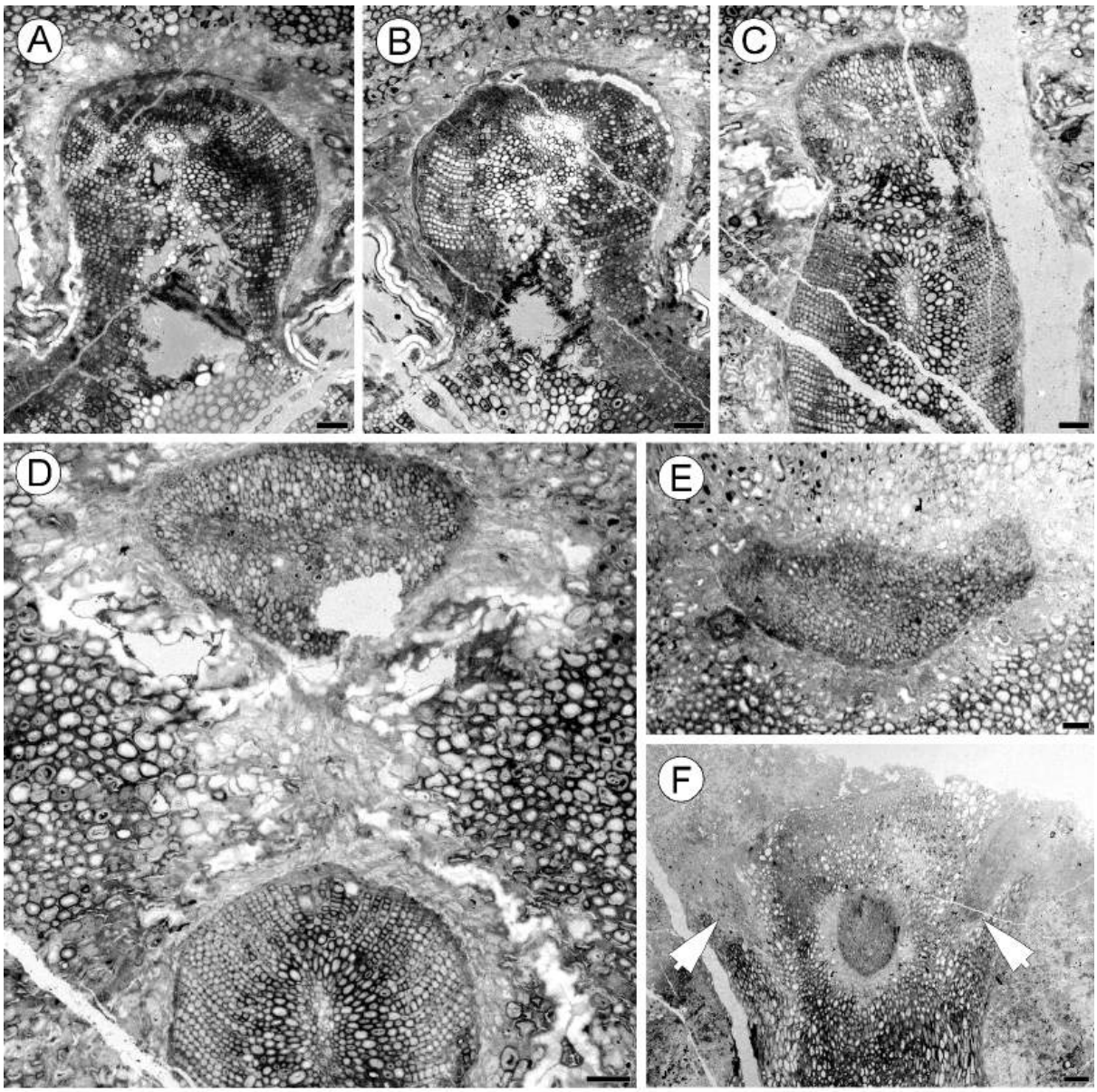

Figure 6: *Stauroxylon beckii,* holotype. Anatomy of trace emission. (A) T-shaped protoxylem strand; that strand corresponds to the upper rib in Figure 4E, 5E; scale bar = 200 µm; slide MN 218-AI 02. (B) Radial division of the protoxylem strand; that strand corresponds to the upper rib in Figures 4F, 5F and the secondary xylem stop surrounding the upper part of the rib; scale bar = 200 µm; slide MN 218-AI 01. (C) Last stage of emission before the trace detaches from the stele; that trace corresponds to the right rib in Figure 4B, 5B; scale bar = 200 µm; slide MN 218-AI 02. (D) Triangular shaped trace; the protoxylem strand is not abaxially or adaxially placed, this trace is emitted by the right rib of Figure 4C, 5C, and a similar trace is emitted by the opposite rib; scale bar = 200 µm; slide MN 218-BS 01. (E) Arc-shaped trace; the protoxylem strand is not abaxially or adaxially placed, this trace is emitted by the right ribs of Figure 4E, 5E, and a similar trace is emitted by the opposite rib; scale bar = 200 µm; slide MN 218-AI 01. (F) Circular trace with two opposite third order axis traces; arrowheads mark the base of the third order traces. This trace is emitted by the left ribs of Figure 4F, 5F, and a similar trace is emitted by the opposite rib; scale bar = 500 µm; slide MN 218-AI 01.

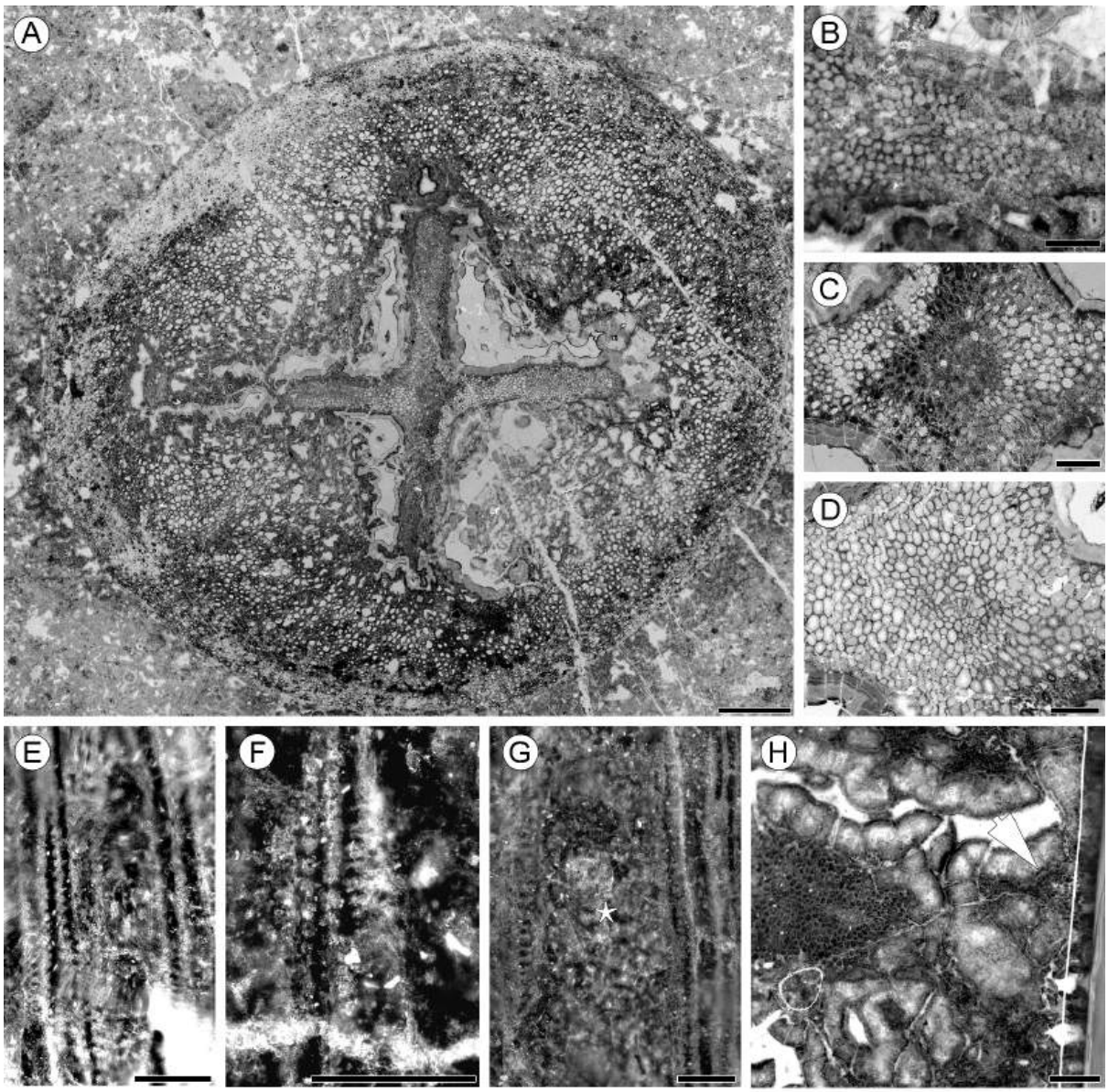

Figure 7: *Stauroxylon beckii*, specimen MN297. (A) Cross section of main axis showing the cruciform actinostele and traces; scale bar = 1 mm; slide MN 297-EI 01; C: Cortex, T: Traces, X1: Metaxylem. (B) Buttonhole-shaped protoxylem strand at the tip of a rib; scale bar = 200 µm; specimen MN 297-B top. (C) Circular central protoxylem strand mainly parenchymatous; scale bar = 200 µm; slide MN 297-EI 01. (D) Central protoxylem strand mainly composed of protoxylem tracheids; scale bar = 200 µm; slide MN 297-FI 01. (E, F) Metaxylem tracheids with round to scalariform pitting (arrows); scale bar = 50 µm; longitudinal section with peel on the specimen MN 297-GL. (G) Protoxylem strand in longitudinal section; note the parenchymatous nature of the inner cells (Pr P) and the annular pitting pattern of the protoxylem tracheids (arrows); scale bar = 50 µm; longitudinal section with peel on the specimen MN 297-GL. (H) Transversal view of the trace (arrowhead); this trace shows the pitting pattern (Figures 7E, 7F, 7G), parenchyma and sclerenchymatous cells (Figures 7G, 8C) in longitudinal section; scale bar = 200 µm; section with peel on the specimen MN 297-G bot.

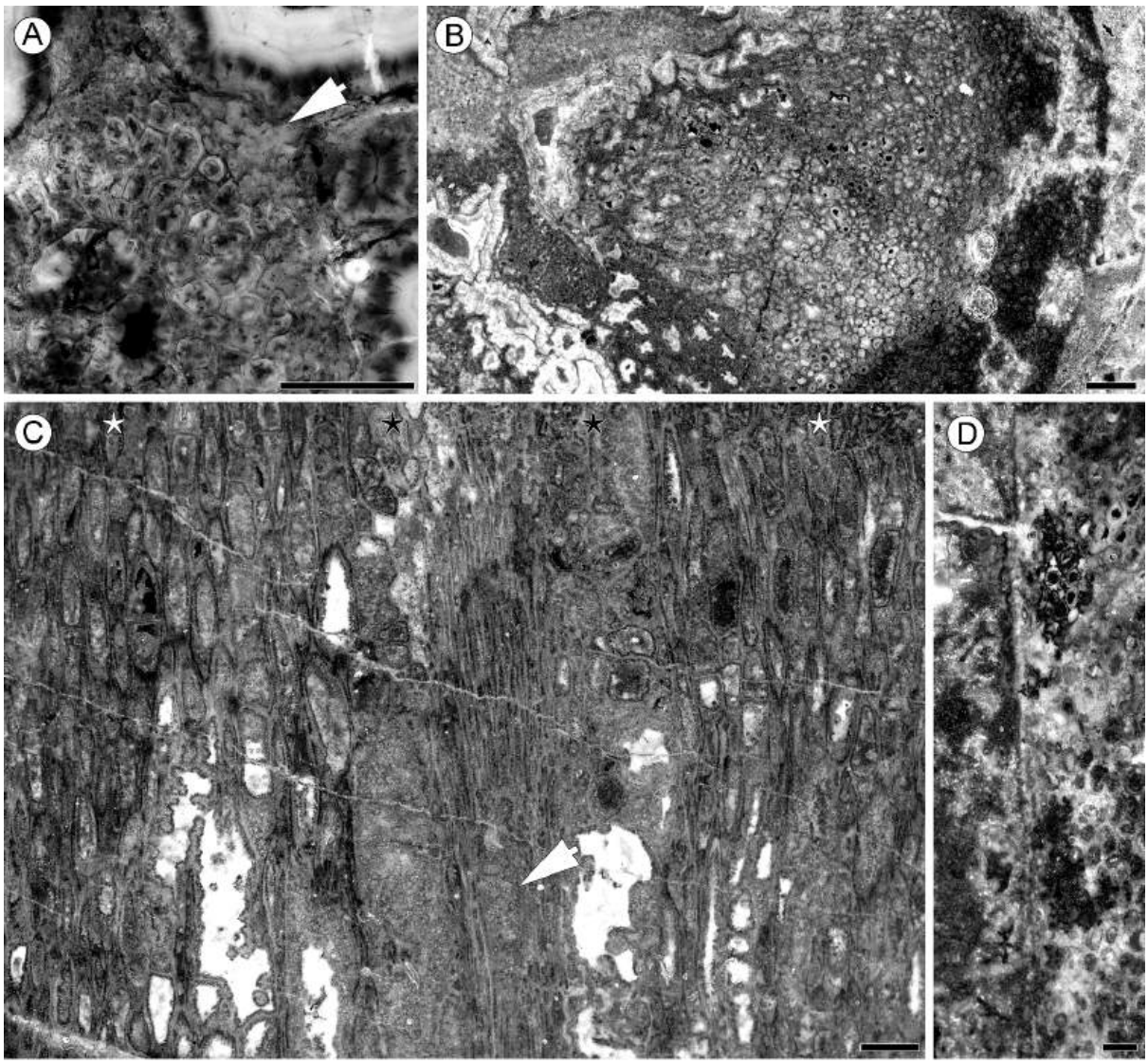

Figure 8: *Stauroxylon beckii*, specimen MN297. (A) Primary phloem (Ph) in transversal section; scale bar = 100 µm; slide MN 297-EI 01. (B) Cortex overview in transversal section; scale bar = 400 µm; section with peel on the specimen MN 297-A3. (C) Longitudinal section with outer cortex (OC), inner cortex (IC), and the metaxylem with parenchymatous protoxylem strand (Pr); note this longitudinal view of the metaxylem is through the trace of Figure 7H; scale bar = 200 µm; longitudinal section with peel on the specimen MN 297-GL 12. (D) Epidermal layer (arrows); scale bar = 100 µm; section with peel on the specimen MN 297-C bot 14.

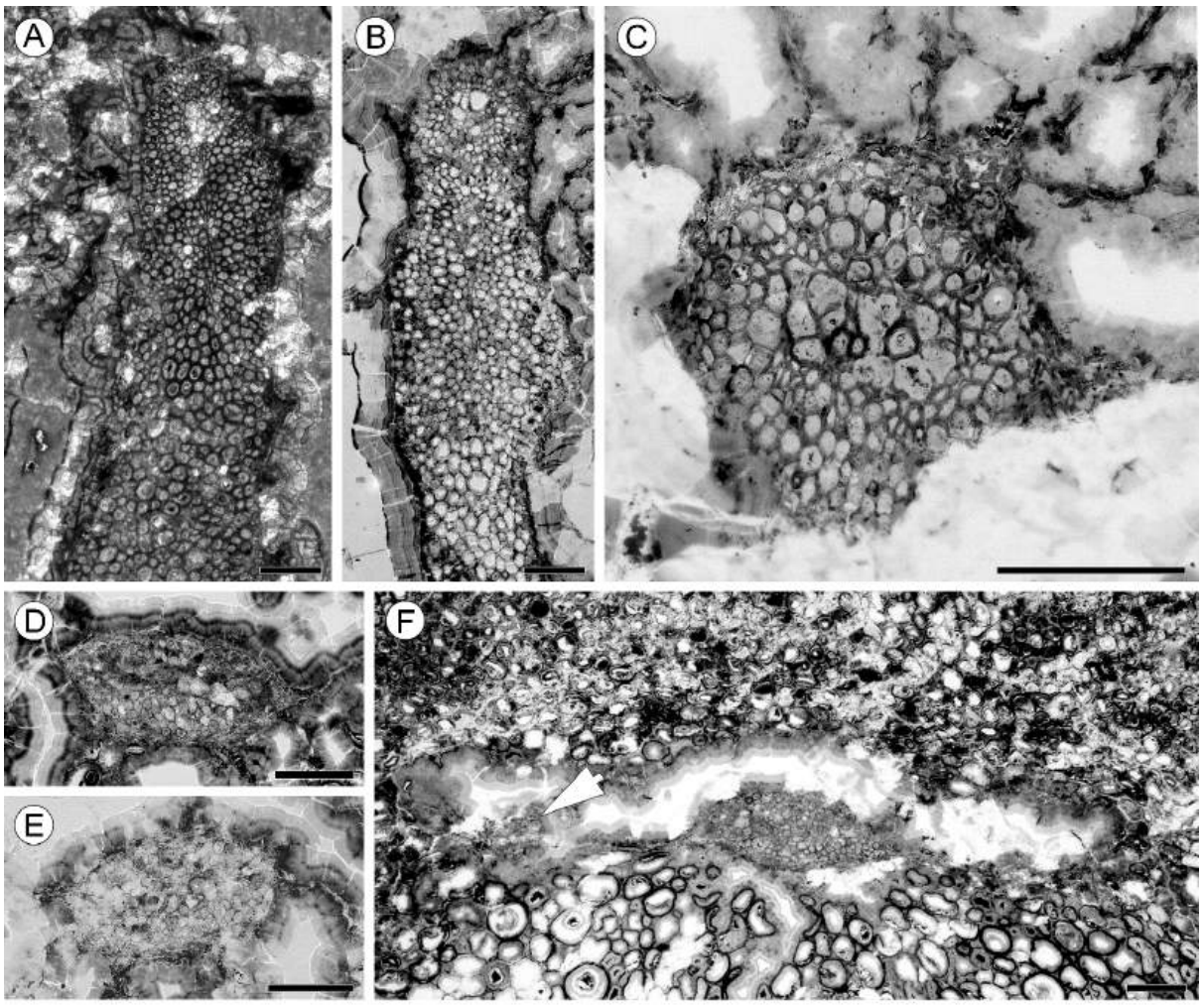

Figure 9: *Stauroxylon beckii*, specimen MN297. Camera lucida drawings of serial transverse sections showing lateral traces emission; scale bar = 2 mm. (A) Polished section MN297-A3. (B) Polished section MN297-A2. (C) Polished section MN297-A1. (D) Polished section MN297-Btop 16. (E) Polished section MN297-Cbot 16; T: Traces, X1: Metaxylem. (F) Polished section MN297-C. (G) Slide MN297- DS 01. (H) Polished section MN297-E. (I) Slide MN297-FI 01.

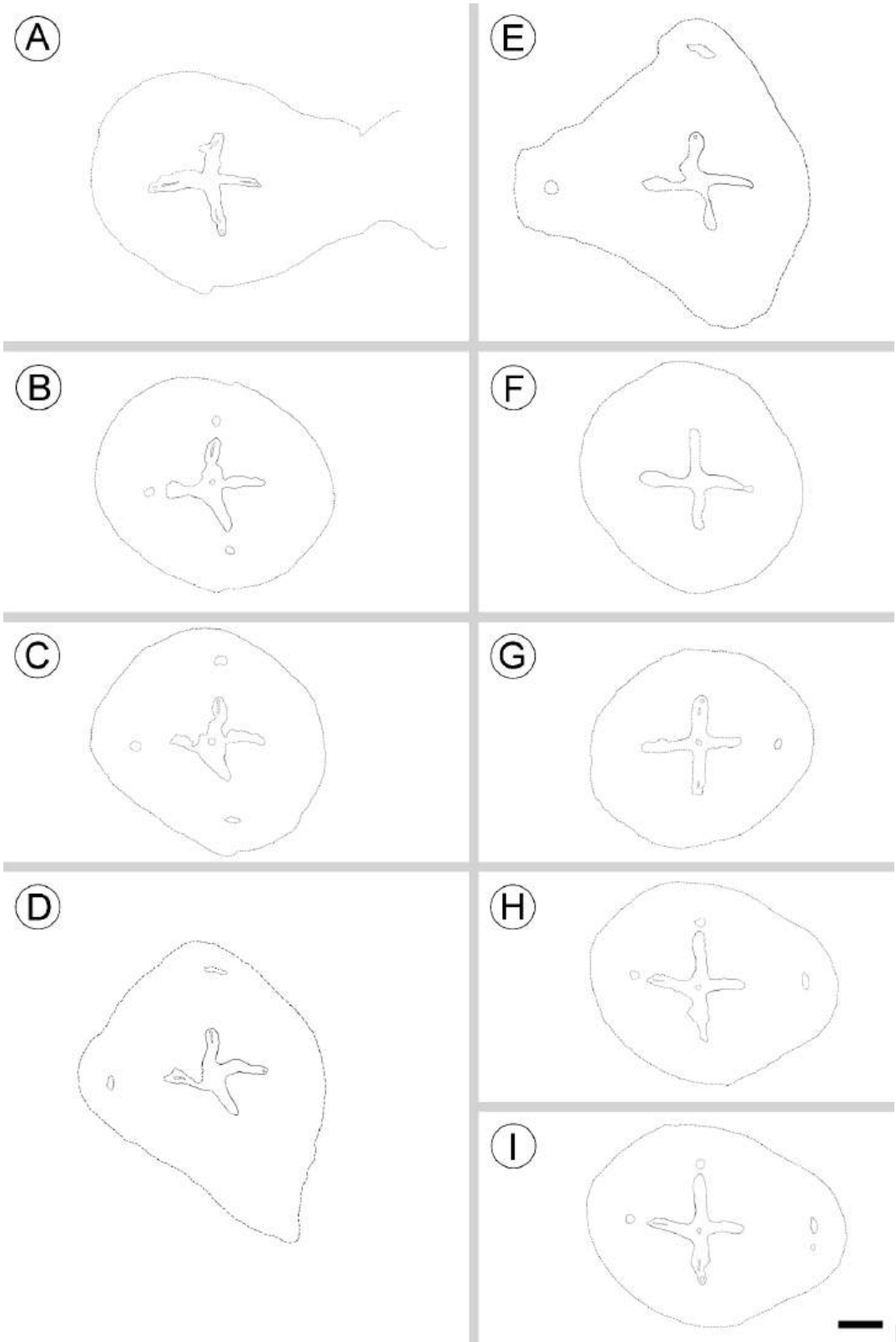

Figure 10: *Stauroxylon beckii*, specimen MN297. Transverse sections corresponding to the drawings on Figure 10; scale bar = 1 mm. (A) Polished section MN297-A3, drawing in Figure 10A. (B) Polished section MN297-A1, drawing in Figure 10C. (C) Polished section MN297-Cbot 16, drawing in Figure 10E. (D) Polished section MN297-C, drawing in Figure 10F. (E) Slide MN297-FI 01, drawing in Figure 10I; C: Cortex, T: Traces, X1: Metaxylem.

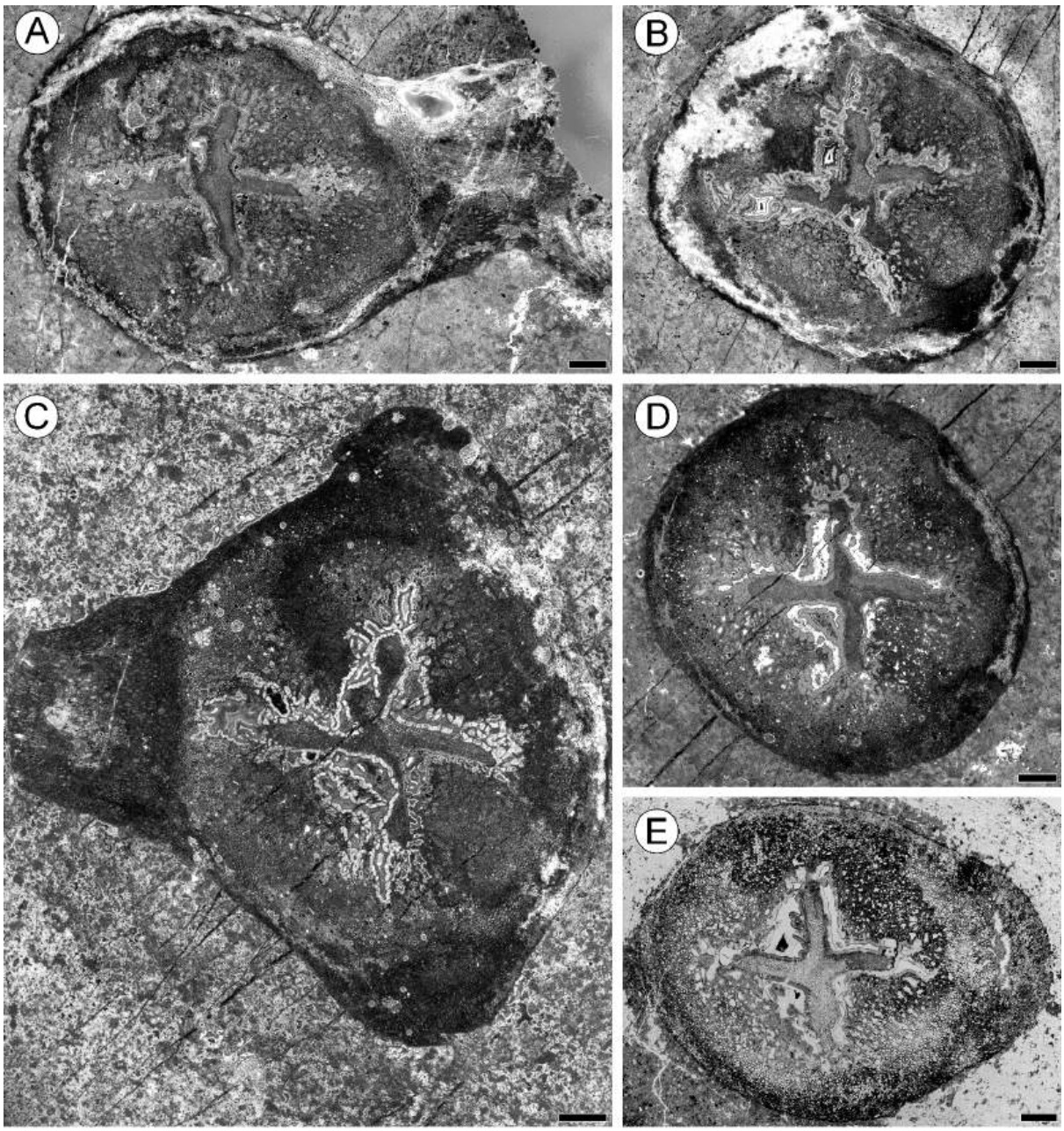

Figure 11: *Stauroxylon beckii*, specimen MN297. Anatomy of trace emission; scale bar = 200 µm. (A) Buttonhole-shaped protoxylem tangentially widened at the tip; peel MN297-FS1. (B) Radial division of the protoxylem strand, with around detaching strand; slide MN 297-EI 01. (C) Circular trace with a large rectangular central protoxylem strand; this trace is emitted by the left rib of Figures 10H, 11E; slide MN 297-FI 01. (D) Tangentially elongated oval trace; the central protoxylem strand form a central band; slide MN 297-EI 01. (E) Tangentially elongated oval trace; the central protoxylem strand looks split in two mesarch strands and this trace is emitted by the right rib of Figure 10G; slide MN 297-DS 01. (F) Oval trace with two opposite third order axis traces; arrowhead mark the basis of the only third order trace preserved, and this trace is emitted by the right ribs of Figures 10I, 11E; slide MN 297-FI 01.

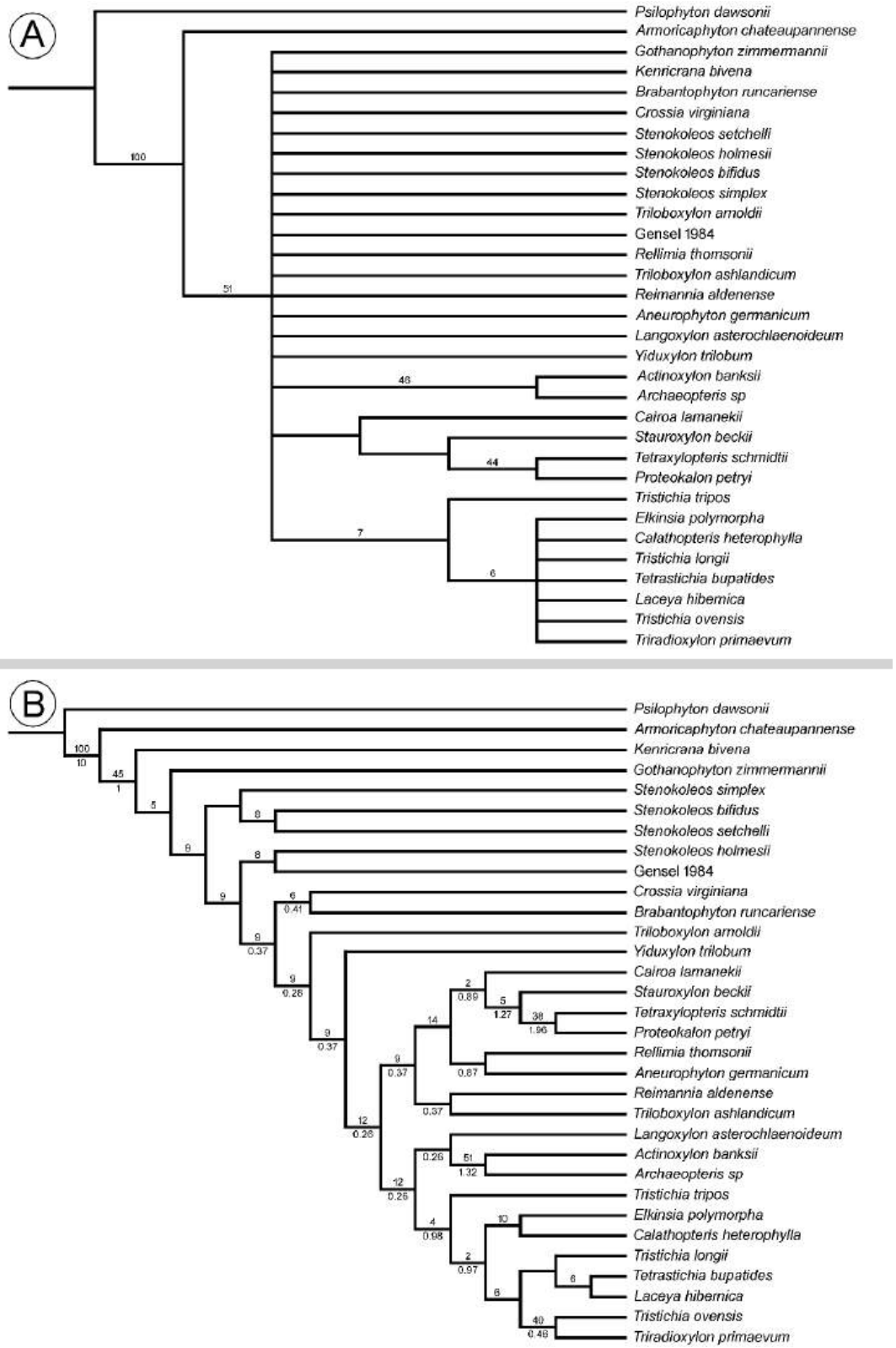

Figure 12: Strict consensus trees of the phylogenetic analyses; numbers at node are bootstrap value ≥2 above and Bremer support ≥0.2 below. (A) Analysis with discrete characters only (32 taxa, 41 characters, 208 most parsimonious trees, length 110, RI = 0.587, CI = 0.436) (B) Analysis with discrete and continuous characters (32 taxa, 50 characters, 1 most parsimonious tree, length 128.797, RI = 0.556, CI = 0.424).

Appendices

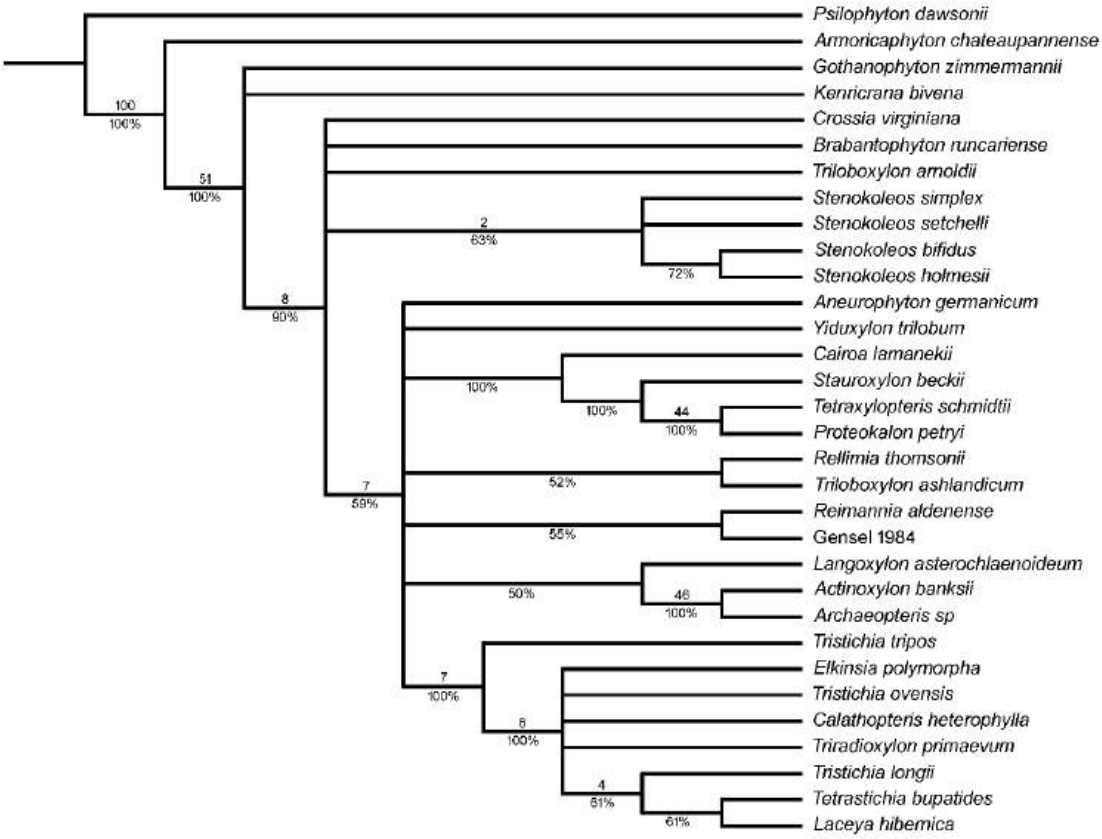

Appendix A1: Analysis with discrete characters only, 50% majority rule tree; numbers at node are bootstrap value ≥2 above and frequency of tree with this node ≥50% below (32 taxa, 41 characters, 208 most parsimonious trees, length 110, RI=0.587, CI=0.436).

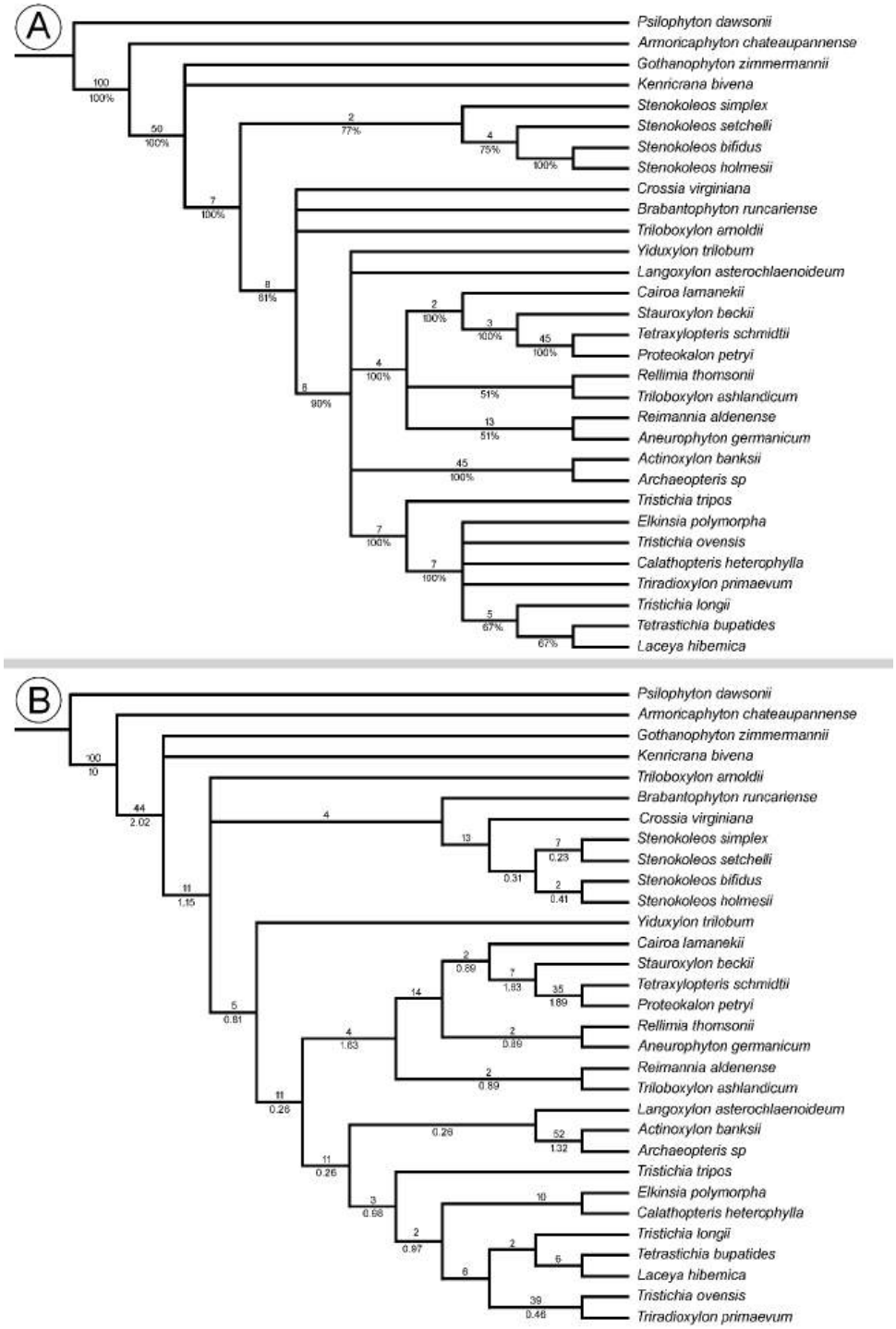

Appendix A2: 50% majority rule trees of analysis conducted without *Wilhowia phocarum*; numbers at node are: for A bootstrap value ≥2 above and frequency of tree with this node ≥50% below and for B bootstrap value ≥2 above and Bremer support ≥0.2 below. (A) Analysis with discrete characters only (31 taxa, 41 characters, 88 most parsimonious tree, length 107, RI = 0.607, CI = 0.449). (B) Analysis with discrete and continuous characters (31 taxa, 50 characters, 3 most parsimonious tree, length 125.519, RI=0.576, CI=0.435).

Appendix A3: Morphological matrix modified from Toledo et al. 2021 TEA ++ version including 50 characters (9 continuous, 41 discrete) and 32 taxa.